IMPACT OF CLIMATE VARIABILITY AND LAND USE CHANGE ON STREAMFLOW IN LAKE CHILWA BASIN, MALAWI

Oscar Clement Kambombe

A Thesis Submitted to the Graduate School in Partial Fulfilment for the Requirements of Master of Science Degree in Water Resources and Environmental Management of Egerton University

EGERTON UNIVERSITY

FEBRUARY 2018

DECLARATION AND RECOMMENDATION

Declaration

This thesis is my original work and has not been submitted for a degree in any other University.

Signature: .... Date: ....

Oscar Clement Kambombe

BM13/14233/15

Recommendation

This thesis has been presented with our approval as university supervisors.

Signature: .... Date: ……………………….........

Prof. Dr. - Ing. Benedict M. Mutua

Division of Planning, Partnerships, Research and Innovation,

Kibabii University

Signature: .... Date: …………………………........

Dr. Vincent O. Odongo

Department of Agricultural Engineering,

Egerton University

COPYRIGHT

DEDICATION

To my mum, dad and siblings for their unwavering love and support; and to my wife Chiko and daughter Noha for enduring many days without me being around

ACKNOWLEDGEMENTSI am so grateful to God Almighty for enabling me to accomplish this work. Special thanks to my supervisors; Prof. Dr.-Ing. Benedict M. Mutua and Dr. Vincent O. Odongo, also Dr. Raphael M. Wambua and the entire Faculty of Engineering and Technology (FET) staff for their guidance and assistance during my study.

My sincere appreciation extends to the Department of Land Resources Conservation under the Ministry of Agriculture, Irrigation and Water Development of Malawi for according me the opportunity to pursue further studies. I am also indebted to Messrs. Gwaligwali, Kamoto, Mwala and Makaika for their field assistance.

Last but not least, this thesis is based on work supported by the United States Agency for International Development, as part of the Feed the Future initiative, under the CGIAR Fund, award number BFS-G-11-00002, and the predecessor fund of the Food Security and Crisis Mitigation II grant, award number EEM-G-00-04-00013.

ABSTRACT

Climate and land use are the two most significant factors that influence watershed hydrology globally. The impact of climate variability on streamflow arises from changes in precipitation and temperature, leading to the adjustment of the physical and biological processes of ecosystems. Land use change impact on streamflow however varies across different regions and environments to warrant a universal theory, making it subject of scientific interest to hydrologists. The aim of this study therefore was to analyse and predict the impact of land use change and climate variability on streamflow in Lake Chilwa basin for the period of existing hydrological records from 1970 to 1999. Four watersheds of Domasi, Likangala, Mulunguzi and Thondwe within the basin were investigated. Land use changes were estimated after processing Landsat images representative of the period under investigation using Remote Sensing (RS) and Geographical Information System (GIS) techniques. Student's t-test was performed to compare the stationarity difference of rainfall and streamflow for the periods; 1970 to 1984 (before land use change) and 1985 to 1999 (post land use change). The probability of exceedance for the two periods were also compared using rainfall duration curves and flow duration curves (FDCs). Furthermore, hydroclimatological trends were tested using Mann-Kendall trend test. Finally, the Soil and Water Assessment Tool (SWAT) model was calibrated and validated to estimate the impact of land use change and climate variability on runoff. Modelling was done only for Thondwe watershed because it had sufficient data required for the exercise. Results from the t-test showed that there was no significant change in rainfall amount for the pre- and post-land use change periods; nonetheless, FDCs revealed that higher runoff characteristics were exhibited in the post-land use change period for watersheds that experienced deforestation and increased agricultural farmlands. The opposite was however the case for the pristine watershed (Mulunguzi) that did not experience severe land use changes. Baseflow trend test results showed a significant decline for the degraded watersheds while for the preserved Mulunguzi watershed, the baseflows were on a significant increase. Modelled results showed that climate variability within Thondwe led to a decline in streamflow by up to 13% while land use change effects increased streamflow by only 3%. From this study, it is concluded that continued degradation is likely to intensify floods and cause extreme low river flows in the basin during rainfall and dry seasons, respectively.

TABLE OF CONTENTS

LIST OF TABLES

LIST OF FIGURES

ACRONYM AND ABBREVIATIONS

AMS	Annual Maximum Series
DEM	Digital Elevation Model
DSMW	Digital Soil Map of the World
ESRI	Environmental Systems Research Institute
FAO	Food and Agriculture Organisation
FDC	Flow Duration Curve
GoM	Government of Malawi
GPS	Global Positioning System
HEC	Hydrologic Engineering Centre
HMS	Hydrologic Modelling System
HRU	Hydrologic Response Unit
ICWE	International Conference on Water and the Environment
ILWIS	Integrated Land and Water Information System
ITCZ	Inter-tropical Convergence Zone
MSS	Multispectral Scanner
NSGEV	Non-Stationary Generalized Extreme Value Model
NSO	National Statistics Office
OLI	Operational Land Imager
OLS	Ordinary Least Squares
OAT	One-factor-At-a-Time
SCS - CN	Soil Conservation Service - Curve Number Method
SRWB	Southern Region Water Board
SSURGO	Soil Survey Geographic Database of the US
SWAT	Soil and Water Assessment Tool Model
TIRS	Thermal Infrared Sensor
UN	United Nations
UNESCO	United Nations Educational, Scientific and Cultural Organisation
UNDP	United Nations Development Program
USACE	United States Army Corps of Engineers
USGS	United States Geological Survey
UTM	Universal Transverse Mercator
WGS	World Geodetic System
WHAT	Web based Hydrograph Analysis Tool

CHAPTER ONE

INTRODUCTION

1.1 Background information

Climate and land use are the two major factors that directly affect watershed hydrology. The effects of climate variability on watersheds largely emanate from alterations in precipitation, caused by changes in other influencing factors such as temperature, wind speed, sunshine hours and relative humidity. Such effects occur at multiple scales and lead to adjustment of the physical and biological processes of an ecosystem (King and Brown, 2006). Changes in land use on the other hand affect the soil infiltration capacity, surface and subsurface flow regimes (Sophocleous, 2002). The effect however is more at the land-water or surface interface (Décamps and Naiman, 1990). Costa *et al.* (2003) observed that the long-term discharge of a river can be modified by decadal or inter-decadal climate variability and by changes in land use.

Studies of land use change impact on watershed hydrology remain of interest to scientists due to the varied hydrological responses observed especially on streamflow generation (Zhang *et al.,* 2008). The variations in streamflow response to land use change are often linked to non-linear relationships, lag effects and limited understanding of the hydrological phenomena, which tends to affect the ability to diagnose the causes (Allan, 2004). Often, significant changes in streamflow due to land use alterations have been observed for smaller watersheds with areas between 1 to 100 km^2 (Kiersch, 2000). Siriwardena *et al.* (2006) suggested that non-uniform variations in land use, variations in forest regeneration, spatial and temporal variation in rainfall over a watershed are some of the factors that lead to varied hydrological conclusions.

The conversion of forest to grassland or to agricultural land for instance, has in some watersheds resulted to a decrease in water yield (Palamuleni *et al.,* 2011; Wang *et al.,* 2006) while in others an increase in water yield has been reported (Andréassian, 2004; Siriwardena *et al.,* 2006). Some studies show increases in both the annual streamflow and/or peakflow volumes due to a reduction in vegetation cover (Bosch and Hewlett, 1982; Bruijnzeel, 1990; Choi and Deal, 2008). These phenomena have been observed in both temperate (Hurkmans *et al.,* 2009) as well as tropical areas (Sang, 2005), although the extent of the increase varies, with smaller watersheds generally showing a more pronounced response. Archer (2003) explains that at small scales, processes such as interception, infiltration and storage dominate whereas channel processes assume a greater role in stream hydrograph as the watershed size increases. Studies conducted for large-scale river watersheds (>100 km^2) usually fail to detect similar relationships that exist for smaller watersheds (Bruijnzeel, 1990).

In general, changes in climate and land use have in recent decades been linked to frequent global occurrences of extreme hydrological events such as floods and droughts (Tian *et al.,* 2011). Study by the Intergovernmental Panel on Climate Change (IPCC) on the effects of climate and land use change on water resources projects a marked reduction in the quantity of water resources in the Southern Africa (Bates *et al.,* 2008). For example, Malawi is among the countries in the Southern Africa region predicted to face serious freshwater challenges despite currently having numerous water resource bodies (GoM, 2013). The annual available water per capita for Malawi was estimated to be 961 m^3 in 1990, with projections estimating a decline to 403 m^3 per capita by 2025 (Hollingworth and Chiramba, 2005).

Based on benchmark indicators developed by Falkenmark and Widstrand (1992) and Gleick (1995), the annual available water per capita below 500 m^3 for a country signifies absolute water scarcity; between 500 m^3 and 1000 m^3 per capita is indicative of water scarcity; and between 1000 m^3 and 1700 m^3 per capita is indicative of water stress while at least 1700m^3 signifies adequacy. From the IPCC projections therefore, Malawi will move from the water scarce to absolute water scarcity category by the year 2025, a situation likely to affect water resource utilisation and wellbeing of the people. The utilisation of water resources in Malawi for irrigation and potable water supply is mostly designed to depend on the provision of little or no water storage (run-of-the-river systems).

Since the run-of-the-river systems, as the case for most supply systems in the Lake Chilwa Basin, rely on unregulated natural river flow, they are highly vulnerable to streamflow variability (Kumambala, 2010). Rivers draining into Lake Chilwa such as Domasi, Likangala, Mulunguzi, and Thondwe are used for potable water supply and also for irrigated farming. Fluctuations and reduction in the quantity and quality of water in these rivers therefore have negative consequences to the people in the basin who depend on these waters for their livelihoods.

While the hydrological impacts of land use change and climate variation occur at all spatial scales, studies at regional and local scales are more relevant to provide important information for local economical and environment protection (Lahmer *et al.,* 2001). Hence accounting for the implications of socio-economic drivers of land use and land cover changes becomes vital for the understanding of hydrological and ecological functions of a river basin (Odongo *et al.,* 2014).

1.2 Statement of the problem

Lake Chilwa Basin has in recent years experienced frequent floods and droughts that have caused social and economic problems (Mvula *et al.,* 2014). There has been recurrent low water supply in the basin in recent years, especially a few weeks preceding the onset of rainy season (Phalombe District Council, 2014). The Southern Region Water Board (SRWB) which supplies potable water in the basin suggested that water levels at abstraction points are becoming low, raising concerns of declining flows of rivers in the basin especially during the dry seasons. However, there has been a knowledge gap on the cause of decline in observed flows especially during the dry seasons and the underlying hydrological processes of the perceived declining river flows.

1.3 Objectives of the study

1.3.1 Broad objective

The broad objective of this study was to analyse and estimate the impact of climate variability and land use change on the streamflows in the Lake Chilwa Basin.

1.3.2 Specific objectives

To address the broad objective the following specific objectives were undertaken:

i. To analyse land use changes in the Lake Chilwa Basin between 1970 and 1999
ii. To evaluate changes in rainfall, streamflow and air temperature characteristics exhibited in the basin between 1970 and 1999
iii. To estimate the separated impacts of land use changes and climate variability on streamflow using the Soil and Water Assessment Tool (SWAT) model

1.4 Research questions

i. What land use changes have occurred in the Lake Chilwa Basin between 1970 and 1999?
ii. What changes are exhibited in rainfall, streamflow and air temperature in the Chilwa basin from 1970 to 1999?

iii. What are the relative and combined contribution of past land use changes and climate variation to changes in streamflows?

1.5 Justification of study

Land use and climate play a vital role in influencing water yield of a watershed. There was limited information however on how changes in climate and land use impacted on the water resources of Lake Chilwa Basin. The Chilwa basin has a population of at least 1.7 million people (GoM, 2008) relying on rivers in the basin for potable water supply and irrigation, mostly on unregulated water supply systems. Reduction and fluctuation of river flow in the basin therefore have a direct impact on water supply for domestic and agricultural purposes. Since the rivers drain into Lake Chilwa, they indirectly provide a source of livelihood to fishermen and communities within the basin. Determining the hydrological response of these rivers to changes in climate and land use therefore is vital for water resource management and land use planning.

Previous studies (e.g. Chavula, 2000; Njaya *et al.,* 2011) conducted in the Chilwa Basin did not analyse trends in river flows and their influencing factors. Study by Chavula (2000) for instance, based on general circulation model (GCM) and global projections which suggest that temperature will increase by 2.6 to 4.7 °C by the year 2075 due to greenhouse gas emissions, concluded that rainfall will continue to exhibit intense variability with increase in floods and droughts in the Chilwa Basin. Njaya *et al.* (2011) on the other hand focused on the environmental dynamics of Lake Chilwa in relation to fish ecology. This study therefore provides insights towards understanding the water yield due to climate variability and land use changes in the Chilwa Basin.

1.6 Scope and limitation

This study focused on the impacts of climate and land use change on streamflow (water quantity). In addition, the research only considered gauged river watersheds with data spanning at least 10 years. Available data for most rivers in the basin was from 1970 to 1999. There was no observed streamflow data between the year 2000 and 2013 for the four watersheds analysed. To quantify the relative and combined contribution of climate and land use change on streamflow using SWAT model, Thondwe watershed was used to demonstrate this because the model required daily rainfall (mm) and maximum and minimum temperatures (°C) as basic inputs in daily time scale, which were not available for the other watersheds. The other watersheds had monthly time scales data only.

CHAPTER TWO

LITERATURE REVIEW

2.1 Climate change and climate variability

According to FAO (2012), climate change refers to a statistically significant variation in either the mean state of the climate or in its variability, persisting for an extended period (typically a decade or longer). Although its perceived effects may not be easily separated from that of climate variability, climate change is slow and gradual unlike year-to-year variability and hence very difficult to perceive without long term scientific records. Climate variability is about yearly oscillations or the difference between the instantaneous state of climate system above or below the mean state computed over many years representative of the era under consideration (Hurrell and Deser, 2010).

2.2 Impact of climate variability on water resources

Recent studies suggest that total flows, probability of extreme high or low flow conditions, seasonal runoff regimes, water quality and the interaction of ground and surface water could all be significantly compromised by climate variability over the coming decades (Kumambala, 2010). Changes in climate and land use coupled with population growth compromise freshwater availability. Rayne and Forest (2013) observed that average water supply per capita between the year 1962 and 2011 declined by 54% world wide and 75% in the sub-Saharan Africa over the same period.

2.3 Impact of land use change on hydrology

Changes in land use affect the overall characteristics and functions of a watershed. Alteration in the agricultural farming pattern or land management can influence flood generating processes and modify flood frequency or magnitude (Svennson *et al.*, 2006). Hydrologic response is an integrated indicator of watershed conditions and climatic influence. These influences are more pronounced on smaller watersheds and attenuate as the watershed size increases. Studies have revealed that direct and powerful linkages exist among spatially distributed watershed properties and watershed processes (Miller *et al.*, 2002).

According to Palamuleni *et al.*(2011), in the short-term, land use change may disrupt the hydrological cycle through increasing, diminishing or totally eliminating low flows in some circumstances. These changes have been observed in watersheds with different sizes ranging from less than 1 km^2 to over 1000 km^2 (Brown *et al.*, 2005).

2.4 Detection of non-homogeneity in hydro-meteorological record

The double mass curve is a useful method for detecting non-homogeneities in a record through a plot of cumulative values of one variable against another during the same time period (Munyaneza, 2014). By plotting cumulative data values of two quantities, the slope can be determined which represents the constant of proportionality between the two quantities. The point of inflection in slope provides an estimate of the time at which a change in land use occurred. As long as the hydrological response does not change, the slope becomes a straight line.

Palamuleni *et al.* (2011) used double mass curve in their study to evaluate land cover change and its impact on Shire River Catchment. Odongo *et al.* (2015) also used double mass curve to detect a change in land cover in a study on characterization of hydro-climatological trends and variability in the Lake Naivasha basin, Kenya. Apart from the double mass curve, singe curve analysis is also used in detecting non-homogeneity of a hydro-meteorological record. Single curve analysis of cumulative values of a single variable over a given time period provides an indication of point of change, given by:

$$X(t) = \sum_{i=1}^{t} P_{ui,} \tag{2.1a}$$

$$Y(t) = \sum_{i=1}^{t} Q_{ui} \tag{2.1b}$$

Where:

$X\ (t)$ = cumulative annual precipitation *(mm)*

$Y\ (t)$ = cumulative flows (m^3)

P_{ui} = Annual precipitation for the year *i (mm)*

Q_{ui} = Total flow for the year *i* (m^3)

2.5 Analysis of trends

Detecting time-series trends exhibited in hydro-meteorological data such as precipitation and streamflow requires statistical methods. Understanding these trends is vital for water resource planning and assessing climate variability impacts on the resource (Xia *et al.,* 2004). Parametric and nonparametric tests have been used by a number of researchers in the detection of time-series trends of hydro-meteorological data. It is revealed that parametric tests present better results and are more powerful than non-parametric (Munyaneza, 2014). However, an implicit assumption of normality that is seldom satisfied with most hydrological data is made (Sharif and Burn, 2009). For instance, Delgado *et al.* (2010) compared a parametric test which accounts for normality of the data, thus non-stationary generalized extreme value model (NSGEV) and a nonparametric method (Mann-Kendall test) together with ordinary least squares (OLS) to detect trends in discharge data for the Mekong River in South East Asia. The authors found out that the NSGEV was a better method to detect trends, followed by the Mann-Kendal test and finally linear regression (OLS).

Although Mann-Kendall is not as powerful as NSGEV, it is widely implemented in many studies for trend detection in hydro-meteorological data such as discharge and precipitation (Adnan and Atkinson, 2010). This is so because the Mann-Kendall test allows investigation of gradual trends without assuming any particular distribution. More importantly, it is less influenced by outliers in the dataset (Hu *et al.,* 2011). It is as well simple to use and capable of handling missing data distributions and robust to the effects of gross data errors (Kahya and Kalayci, 2004). The Mann-Kendal test is given by:

$$S = \sum_{k=1}^{n-1} \sum_{j=k+1}^{n} \operatorname{sgn}(x_j - x_k) \qquad (2.2)$$

Where:

x_j and x_k = Annual values in years j and k, ($j > k$)

$$\operatorname{sgn}(x_j - x_k) = \begin{cases} 1 & if\ (x_j - x_i) > 0 \\ 0 & if\ (x_j - x_i) = 0 \\ -1 & if\ (x_j - x_i) < 0 \end{cases} \qquad (2.3)$$

When S is greater than 0, it implies a positive trend, and a negative S indicates a decreasing trend. The S is approximately normally distributed for n ≥ 8, with the mean and variance given as:

$$E(S) = 0 \qquad (2.4)$$

$$VAR(S) = \frac{1}{18}\left[n(n-1)(2n+5)\right] \qquad (2.5)$$

When tied ranks exist in the data, the statistic $S = 0$ and variance of S, $Var(S)$ is calculated by:

$$VAR(S) = \frac{1}{18}\left[n\,(n-1)(2n+5) - \sum_{p=1}^{q} t_p (t_p - 1)(2t_p + 5)\right] \qquad (2.6)$$

Where:

q = number of tied groups

t_p = number of data values in the p^{th} group

The test statistic Z is calculated using the values of *S* and *VAR(S)* given by:

$$Z = \begin{cases} \frac{S-1}{\sqrt{VAR(S)}} & if\ S > 0 \\ 0 & if\ S = 0 \\ \frac{S+1}{\sqrt{VAR(S)}} & if\ S < 0 \end{cases} \qquad (2.7)$$

Where:

Z = standardised Z value

S = test statistic

VAR(S) = variance

The standardised *Z* value is used to determine the significance of any trend in the data set. The null hypothesis stating that there is no trend is rejected if $|Z_c| > Z_{1-\alpha/2}$, at a significance level α that indicates the trend strength.

2.5.1 Sen's slope estimator

The Sen's slope method is a technique used to estimate the magnitude of monotonic trends in *N* pairs of data (Grocic and Trajkovic, 2013). A monotonic upward or downward trend for a variable implies that there is a consistent increase or decrease in the variable through time, but the trend may or may not be linear (Hirsch *et al.*, 1982). The Sen's slope is given by:

$$Q_i = \frac{x_j - x_k}{j - k}\ for\ i = 1, ..., N, \qquad (2.8)$$

Where:

Q_i = Sen's slope

x_j and x_i = data values in years *j* and *i*, (1 < j < i < n)

A positive Q_i value indicates an upward trend while a negative value indicates a downward trend.

2.6 Land use change analysis

The analysis of land use change has become an area of interest to environmentalists, conservationists and land use planners due to its impact on natural ecosystems (Halmy *et al.*, 2015). A number of techniques are available for land use change detection that use digital imagery such as airborne scanners, digital orthophotography and satellite imagery (Jensen and Toll, 1982; Martin, 1986; Green *et al.*, 1994). Landsat images in particular have mostly been used in the classification of different landscape components (Ozesmi and Bauer, 2002; Butt *et al.,* 2015).

2.6.1 Image classification

Classification of remotely sensed satellite images provides fundamental information on characteristics, activities and status of specific areas of the earth's surface (Enderle and Weih, 2005). It involves clustering pixels on the image to a particular spectral class thereby providing information on the type of land use in the study area (Janssen and Gorte, 2004). Image classification is aimed at converting image data to thematic data and is performed using a remotely-sensed image to make use of its multispectral information (Adnan and Atkinson, 2010).

2.6.2 Unsupervised and supervised classification

The supervised classification is one of the techniques commonly used in satellite image classification. This process of supervised classification involves initially undertaking the unsupervised classification. During the unsupervised classification, image pixels are clustered into groups of unlabeled classes (Abburu and Golla, 2015). In this process, the computer software such as Image Analyst extension in ArcGIS automatically groups the image pixels into separate clusters depending on their spectral features. An expert later assigns land cover type to each cluster in a process called supervised classification.

In supervised classification, the specialist has to recognize conventional classes (real and familiar) or meaningful classes in a scene from prior knowledge. Such knowledge may include personal experience with the region, experience with thematic maps, or by on-site visits (Short, 2005). This familiarity allows the specialist to choose and set up discrete classes called training sites. Training sites represent each known land cover category that appears fairly homogeneous on the image determined by similarity in tone within shapes delineating the category. The advantage of this technique is that the analyst has full control of categories or classes to be assigned in the final classification (Enderle and Weih, 2005).

2.7 Hydrological modelling

Use of hydrological models is vital in guiding decision making such as formulation of water resource policy, regulation and management plans (Magoma, 2009). Hydrological models are used to quantify runoff, base flow, water balance and sediment yield among others. These models can be categorized into lumped, semi-distributed or distributed (Durand *et al.*, 2002). Lumped models do not consider in much detail the spatial distribution of physical properties such as soil, land use or topography and therefore are not as accurate as distributed models.

The advantage of lumped over distributed models is that they require less data and limited number of parameters (Montanari *et al.*, 2006). Semi-distributed and distributed models require numerous parameters because they represent space by sub-basins or hydrological response units (HRUs). Hydrological models mimic the natural processes of a water cycle. They consist of equations, often based on the physical premises, whose parameters are specific for the selected watershed and problem of study (Bárdossy, 2007). Some of these models include the Hydrologic Model System (HEC-HMS) and the Soil and Water Assessment Tool (SWAT).

2.7.1 HEC-HMS

The Hydrologic Modelling System (HMS) is a rainfall-runoff model developed by the Hydrologic Engineering Center (HEC) of the United States Army Corps of Engineers (USACE). HEC-HMS is a lumped, semi-distributed software package used to simulate rainfall-runoff processes in a watershed or region (Munyaneza, 2014). According to USACE (2000), HEC-HMS requires three input components namely;

a) Basin component, which is a description of different elements of the hydrologic system comprising sub-basins, channels, junctions, sources, sinks, reservoirs and diversions including their hydrologic parameters and topology;

b) Meteorological component, which is a description in space and time of the precipitation event to be modelled. It consists of time series of precipitation at specific points or areas and their relation to the hydrologic elements; and

c) Control specifications component, which defines the time window for the precipitation event and for the calculated flow hydrograph (USACE, 2000).

The HEC-HMS is good for carrying out both the event and continuous based simulations, in addition to modelling of large river basin water supply, flood hydrology, and small urban or natural watershed runoff (USACE 2009). The limitation of using this tool however includes its inability to model looping or branching networks. Besides, the model code for HEC-HMS model is not publicly available (Yilmaz, *et al.*, 2011)

2.7.2 SWAT Model

The Soil and Water Assessment Tool (SWAT) model has been applied by a number of researchers in different parts of the world, under different climatic and management conditions (Ma *et al.,* 2015). SWAT is a semi-distributed, physically based and computationally efficient hydrological model which allows the simulation of a number of different physical and hydrological processes occurring across a watershed. It can simulate a number of watershed processes such as streamflow and sediment yield (Neitch *et al.,* 2005). In the SWAT-modelling approach, a watershed is divided into a number of sub-basins. Each sub-basin is further divided into groups of similar soil and land cover areas called Hydrological Response Units (HRUs) as described by Arnold and Fohrer (2005).

The SWAT model provides two infiltration methods for estimating the surface runoff volume component from the HRUs namely; the SCS-curve number (CN) method (USDA-SCS, 1972) or the Green & Ampt infiltration method (Green and Ampt, 1911). Whereas the CN-method uses daily rainfall rates, the Green & Ampt technique requires smaller time-steps to properly simulate the infiltration process. On the other hand, the surface runoff is modelled in SWAT using the SCS curve number method given by:

$$Q_{surf} = \frac{(R_{day} - I_a)^2}{(R_{day} - I_a + S)} \tag{2.9}$$

Where:

Q_{surf} = accumulated runoff or rainfall excess *(mm)*

R_{day} = rainfall depth for the day *(mm)*

I_a = initial abstractions (usually taken as equal to $0.2S$)

S = retention parameter *(mm)*

The retention parameter *S* is defined by:

$$S = 25.4\left[\frac{1000}{CN}\right] - 10 \quad (2.10)$$

Where:

CN = curve number

The merits of using SWAT include its availability as an open source tool. In addition, SWAT has a detailed online documentation, user groups, video tutorials, international conferences and a unique literature database available for reference (Cambien, 2017); making it user-friendly and widely used tool for modelling watershed scale hydrological processes (Gassmann *et al.,* 2010; Refsgaard *et al.,* 2010; Varga *et al.,* 2016). The SWAT model was hence selected for this study.

2.8 SWAT Model inputs and application procedure

Application of SWAT model uses the ArcSWAT which is the model interface in ArcGIS. The input to the model for rainfall-runoff simulation is geographic data in form of digital elevation model (DEM), soil and land use data, subsurface parameters and weather data driving the dynamic hydrological processes. The geographic data, according to Koch and Cherie (2013), is often prepared in a GIS environment (projections and orientations) and then used as input into the model (ArcSWAT). The simulated outputs of the SWAT model include surface runoff, infiltration, evapotranspiration (ET), lateral flow, percolation to shallow and deep aquifers and channel routing (Arnold *et al.,* 1998). The procedure for simulating runoff is shown in Figure 2.1, adapted from Principe and Blanco (2013).

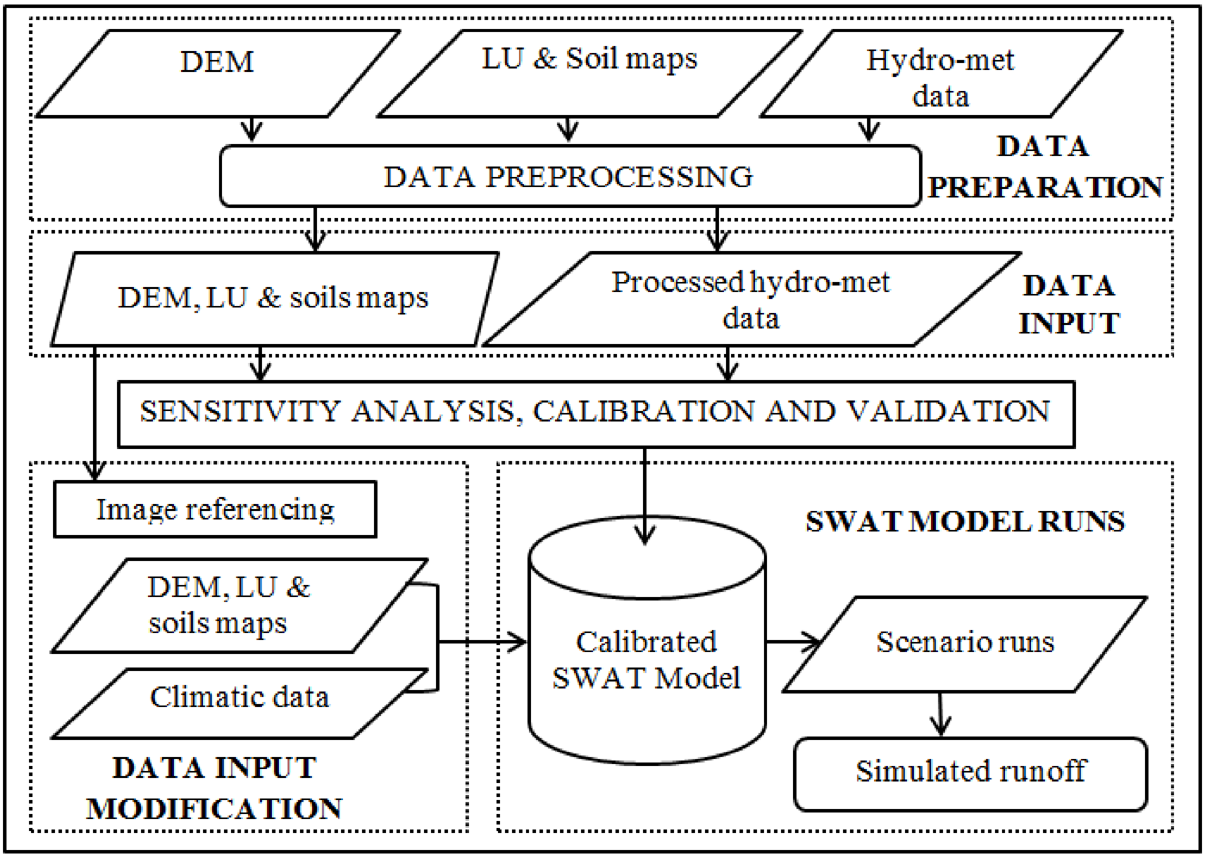

Figure 2.1: SWAT application procedure

2.9 Sensitivity analysis

Sensitivity analysis is the process of determining the rate of change in model output with respect to changes in model inputs (parameters). Local and global sensitivity analyses are generally performed to identify key parameters and the parameter precision required for calibration (Ma *et al.*, 2012). Local sensitivity analysis involves changing values one-at-a-time while global allows all parameter values to change simultaneously. However, the two analyses may yield different results.

Sensitivity of one parameter often depends on the value of other related parameters; hence, the problem with one-at-a-time analysis is that the correct values of other parameters that are fixed are never known (Koch and Cherie, 2013). The disadvantage of the global sensitivity analysis is that it needs a large number of simulations. Both procedures, however, provide insight into the sensitivity of the parameters and are necessary. Most ArcSWAT versions are based on Latin Hypercube (LH) and a One-factor-At-a-Time (OAT) sampling (Veith and Ghebremichael, 2009).

This means that during the sensitivity analysis, the SWAT-model is run $m*(p+1)$ times, where m is the number of LH loops, and p is the number of hydrological SWAT parameters being evaluated. Hence one LH- loop involves performing $p+1$ model runs to obtain one partial effect for each parameter. Parameter sensitivity is given by:

$$PS_{ij} = \frac{\dfrac{\left| O(x_1,..., x_i + \Delta x_i,..., x_n) - O(x_1,..., x_i,..., x_n) \right|}{O(x_1,..., x_i + \Delta x_i,..., x_n) - O(x_1,..., x_i,..., x_n)}}{\left| \Delta x_i \right|_{/x_i}} \tag{2.11}$$

Where:

PS_{ij} = the relative partial effect of parameter x_i around the LH point j

P = the number of parameters

O = the objective function (model output)

ArcSWAT 2012 has the ability to automatically perform global sensitivity analysis and rank best parameters. The global sensitivity analysis was therefore used in this study despite its demand for a large number of simulations.

2.10 Model calibration

Calibration of a model is a process where the model parameter values are adjusted so that the model agreement with respect to a set of experimental data is maximized (Trucano *et al.*, 2006). The SWAT input parameters are process based and must be held within a realistic uncertainty range (Arnold *et al.*, 2012). This ensures that the model closely simulates the behavior of a watershed in terms of its response to inputs such as rainfall. Model calibration is performed by carefully selecting values for model input parameters (within their respective uncertainty ranges) by comparing model predictions or output for a given set of assumed conditions with observed data for the same conditions.

Conventionally, calibration is performed manually and consists of changing model input parameter values to produce simulated values that are within a certain range of the measured data (Balascio *et al.*, 1998). However, when the number of parameters used in the manual calibration is large, especially for complex hydrological models, manual calibration can become labour intensive. However, calibration can be accomplished manually or using auto calibration tools in some models such as ArcSWAT (Van Griensven and Bauwens, 2003; Van Liew *et al.*, 2005).

The SWAT Calibration and Uncertainty Program (SWAT - CUP) is one of the programs that is used for auto calibration of SWAT model. SWAT-CUP is a standalone program that links to the SWAT's output text file, the TxtInOut (Rouholahnejad *et al.,* 2012). The program uses calibration algorithms such as the Generalized Likelihood Uncertainty Estimation (GLUE) (Beven and Binley, 1992), Sequential Uncertainty Fitting (SUFI2) (Abbaspour *et al.*, 2004), Parameter Solution (ParaSol) (Van Griensven and Meixner, 2006) and Markov chain Monte Carlo (MCMC) (Kuczera and Parent, 1998). The SUFI2 is commonly used for SWAT rainfall-runoff modelling and was therefore used in this study.

2.11 Model validation

The process of model validation demonstrates whether a given site-specific model is capable of making sufficiently accurate simulations (Refsgaard, 1997). Validation involves running a model using parameters that were determined during the calibration process and comparing the simulation to observed data not used in the calibration. According to Arnold *et al.* (2012), a good model calibration and validation should ensure that other important model outputs are reasonable and are verified. Graphical and statistical methods with some form of objective statistical criteria are used to determine when the model has been calibrated and validated.

The Nash and Sutcliffe (1970) test of model efficiency *(NS)*, the coefficient of determination (R^2), percent bias *(PBIAS)* and root mean square error-observations to standard deviation ratio *(RSR)* are used to assess the predictive power of the SWAT model (Li *et al.*, 2009). The equations are given as follows:

$$NS = 1 - \frac{\sum_{i=1}^{n}(Q_{obs} - Q_{sim})^2}{\sum_{i=1}^{n}(Q_{obs} - \overline{Q}_{obs})^2} \tag{2.12}$$

Where:

Q_{obs} = measured streamflow

Q_{sim} = simulated streamflow

The calculated *NS* value ranges from -∞ to 1, with *NS* = 1 indicating best model prediction (optimal). Values between 0 and 1 are generally considered as acceptable levels of model performance, whereas values < 0 indicate that the observations mean is a better predictor than the estimated value, which implies unacceptable model performance (Krause *et al.*, 2005; Moriasi *et al.*, 2007).

$$R^2 = \frac{\left[\sum_i \left(Q_{obs\,i} - \overline{Q}_{obs}\right)\left(Q_{sim\,i} - \overline{Q}_{sim}\right)\right]^2}{\sum_i \left(Q_{obs_i} - \overline{Q}_{obs}\right)^2 \sum_i \left(Q_{sim_i} - \overline{Q}_{sim}\right)^2} \tag{2.13}$$

The R^2 statistic can range from 0 to 1, where 0 indicates no correlation and 1.0 represents perfect correlation (Abbaspour, 2013)

$$PBIAS = \frac{\sum_{i=1}^{n} (Q_{obs} - Q_{sim})}{\sum_{i=1}^{n} Q_{obs}} \tag{2.14}$$

The optimal value of *PBIAS* is 0. Low magnitude values close to the 0 value indicate good model simulation performance. Positive values indicate model underestimation bias and negative value indicate model overestimation bias.

$$RSR = \frac{\sqrt{\sum_{i=1}^{n} (Q_{obs} - Q_{\sin})^2}}{\sqrt{\sum_{i=1}^{n} (Q_{obs} - \overline{Q_{obs}})^2}} \tag{2.15}$$

$$= \frac{RMSE}{STDEV_{obs}}$$

The value of 0 represents best model performance. When the value of *RSR* is equal to 0, it indicates that there is no residual variability and therefore good model simulation (Li *et al.*, 2009). The smaller the *RSR value*, the better the model simulation performs.

2.12 Other studies conducted using SWAT

Zhang *et al.* (2012) applied the SWAT model to assess the impacts of climate change and human activities on runoff for the Huifa River in China. Their study revealed that both climate change and human activities were responsible for the decrease of observed Huifa River streamflow. Human activities however, accounted more to the reduction in flow due to water regulation and storage projects.

In Africa, SWAT model has also been used by a number of researchers. For instance, Githui (2009) examined historical land use and climate change in a large river basin for Nzoia River watershed in Kenya with an area of 12, 709 km^2. The study revealed that without climate change, land cover change would account for a difference in runoff of about 55% to 68%. On the other hand, climate change without land cover change accounted for a difference in runoff of about 30% to 41%. In another study, Sang (2005) SWAT model in Nyando Basin in Kenya and determined that an increase of rainfall by 15% would increase peak flow from $111m^3s^{-1}$ to $159m^3s^{-1}$. Magoma (2009) examined the applicability of SWAT in the Rugezi wetland catchment in Rwanda (197 km^2). He found out that the simulated flows complied with the measured flows.

CHAPTER THREE

METHODOLOGY

3.1 The study area

Lake Chilwa Basin is located in Southern Malawi within latitudes 14° 40′ S and 15° 55′ S and longitudes 35°15′ E and 35° 45′ E. It has a watershed area of 8,349 km^2 with 5669 km^2 (68%) in Malawi and 2680 km^2 (32%) in Mozambique (Mvula *et al.*, 2014). The lake area is about 683 km^2. The basin consists of the Phalombe, Zomba and Machinga Districts on the Malawi side and part of Mozambique on the eastern side. The altitude ranges from about 500 m above mean sea level (a.m.s.l) close to the lake shores to about 2650m (a.m.s.l) around Zomba and Mulanje Mountains. The map of Lake Chilwa Basin is presented in Figure 3.1.

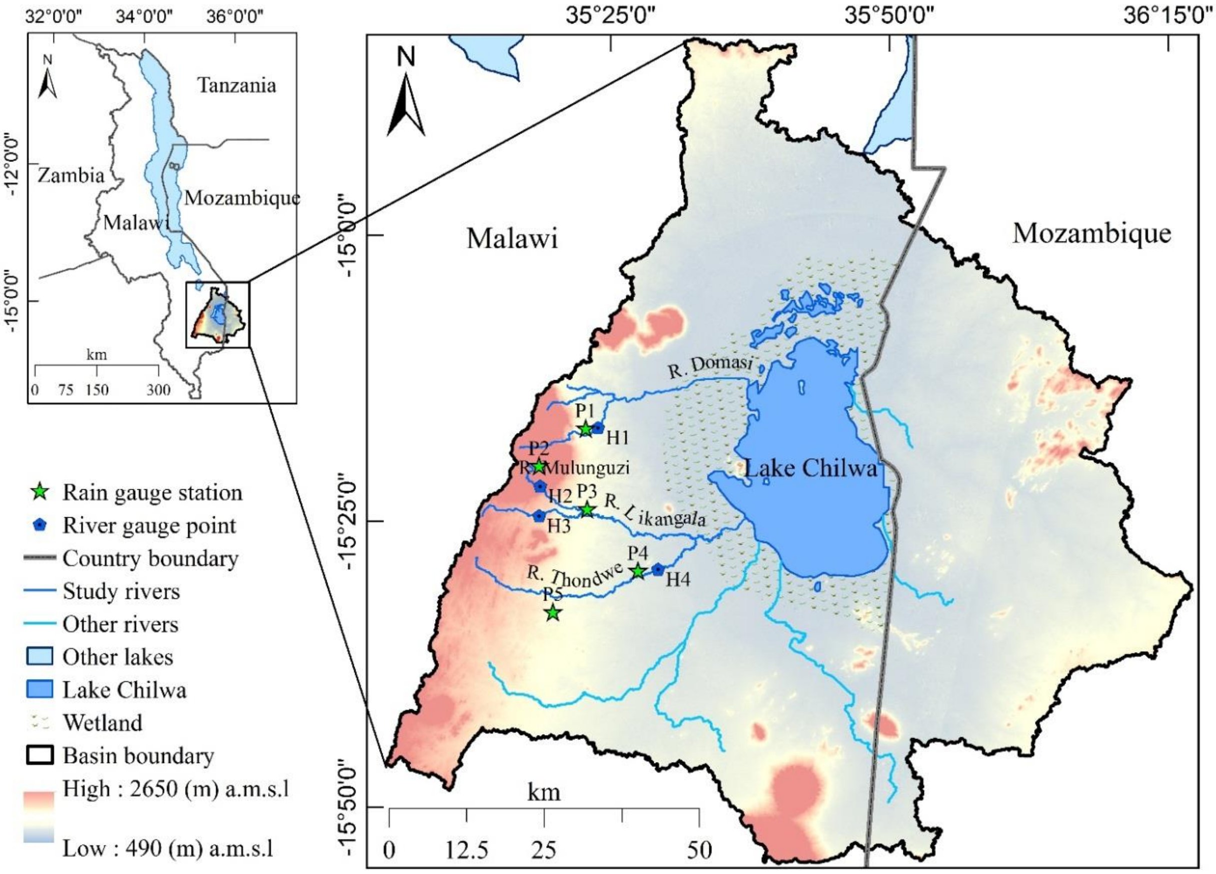

Figure 3.1: Location of Lake Chilwa Basin highlighting the studied rivers and hydrological gauge points/ and or stations

Key:

H1 = Domasi TTC - river gauge point
H2 = Zomba Plateau - river gauge point
H3 = Nkokanguwo - river gauge point
H4 = Jali - river gauge point

P1 = Domasi College rain gauge point
P2 = Zomba Plateau rain gauge station
P3 = Chancellor College gauge station
P4 = Jali rain gauge station
P5 = Makoka rain gauge station

Rainfall distribution ranges from 1100 to 1600 mm per year, reaching more than 2000 mm in Zomba and Mulanje Mountain while in the lowland plains, rainfall ranges between 800 mm and 900 mm per year (Mvula *et al.*, 2014). The rainfall pattern in the basin is unimodal with most rainfall (80%) occurring in the months of November to April. From the months of May to August there are sporadic winter rainfall (locally known as "*chiperone"*) experienced in the highlands.

These winter rains originate from an influx of cool moist south-eastern winds (Ngongondo, 2011). According to the British Geological Survey (2004), the climate in the basin is tropical wet and dry, commonly known as Savanna climate. The rainfall regime is strongly influenced and controlled by the Inter-Tropical Convergence Zone (ITCZ), where the north easterly monsoon and south easterly trade winds converge (Ngongondo, 2011). The mean annual temperature for the Chilwa basin varies from 21 °C to 24 °C (Chavula, 2000).

3.2 Analysis of land use change in the Chilwa Basin

Landsat images were downloaded from the United States Geological Surveys (USGS) website - http://www.earthexplorer.usgs.gov. Topographic maps were obtained from the Department of Surveys of Malawi and the University of Malawi, Chancellor College, Geography Map Library.

3.2.1 Image preprocessing

Two successive Landsat images captured on path 167, rows 70 and 71 covering the entire Lake Chilwa Basin were used in the land use change analysis. Image acquisition dates were 8th October 1973, from the Landsat 1-5 Multispectral Scanner (L 1-5 MSS); 17th September 1994, from the Landsat 4-5 Thematic Mapper (L 4-5 TM); and 5th October 2013 from Landsat 8 Operational Land Imager or Thermal Infrared Sensor (L8 OLI/TIRS). The images were taken at approximately twenty (20) year interval from 1973, with the 2013 image being used for ground-truthing as the most recent. The two successive images for each year were imported into ArcGIS in geo-tiff format and mosaicked into single image stack. Correction of radiometric distortions and geometric orientation of the images was thereafter done, and the images were projected to the universal transverse Mercator (UTM) projection, Zone 36S.

3.2.2 Unsupervised classification

Image Analyst extension in ArcGIS was used to perform the unsupervised classification into eight classes. The image pixels were hence grouped into eight unlabeled clusters based on their spectral signatures. The choice of eight classes for the unsupervised classification was determined to be at least more than the existing dominant land use/cover classes (five) in the basin observed after conducting a reconnaissance survey. The choice of eight classes was stricter so that in the event that there existed more classes not captured during the reconnaissance survey, the three extra classes would be assigned a class set later during supervised classification.

Using the 2013 image, thirty (30) sample points were randomly selected from each cluster (stratified sampling), making a total of 240 sample points that were later physically identified on the ground (ground-truthing). The coordinates (x, y) of the sampled points were then identified and given a distinct identity code for ground-truthing. A map showing the points and their corresponding identity codes as shown in Appendix C2 was eventually produced in ArcMap and later used during the ground-truthing exercise. The coordinates and their given codes for each randomly selected point were then uploaded into a Global Positioning System (GPS) receiver gadget for feature identification on the ground.

3.2.3 Supervised classification

Using waypoint manager tool in the GPS receiver, sample points were physically located. Land use features surrounding each point were observed and recorded in a field notebook. Pictures were also taken in four cardinal directions at each sample point for reference. Using the observed land use features, training sites for the major land uses in the basin were later created, firstly on the 2013 image. Spectral signatures from the classified 2013 image and archive maps were also used to assist in creating training sites for the 1994 and 1973 images. This led to the reclassification of the images (supervised classification) into five major land use classes. Land area in hectares (ha) under each major class was later calculated for the basin and for each watershed.

3.3 Analysis of hydroclimatological characteristics

Rainfall and temperature data were obtained from the Meteorological Department of Malawi while streamflow data was obtained from the Department of Water.

3.3.1 Rainfall amount

Historical rainfall records from 1970 to 1999 for four rain gauge stations of Chancellor College, Domasi, Makoka and Zomba Plateau were used in the analysis. The available rainfall data for Makoka Station was in daily record (mm) while for the other stations was in monthly records (mm). These rainfall datasets were later converted to annual rainfall (mm) by cumulatively adding the values to annual totals and split into two periods from 1970 to 1984 and 1985 to 1999 to compare annual rainfall for the two periods.

The split periods were based on study by Allison *et al.* (2007) that generally showed a decline in lake levels from 1985 to 1999 compared to the period from 1970 to 1984. The hypothetical assumption in this study was that there was no significant hydroclimatological difference between the two periods. Statistical t-test at the 0.05 level of significance (α) was used to compare presence of significant difference between the two periods.

3.3.2 Rainfall patterns

Monthly rainfall record (mm) from 1970 to 1999 was used to assess possible changes in pattern. Plots of seasonal rainfall pattern were then made for the two periods on the same axis. Rainfall patterns for the two periods were then compared for the onset, secession and general distribution. This analysis was done for the four stations of Chancellor College, Domasi, Makoka and Zomba Plateau stations which represented the watersheds of Likangala, Domasi, Thondwe and Mulunguzi, respectively.

3.3.3 Mean annual streamflow

Daily river discharges (m^3s^{-1}) recorded from 1970 to 1999 for Domasi, Likangala, Mulunguzi and Thondwe Rivers were split into two periods from 1970 to 1984 and 1985 to 1999. The datasets were therefore converted to the average annual discharge (cumecs) by dividing cumulative daily flow for each year by the number of days for each particular year. Statistical t-test at 95% level of confidence was used to test for significant difference in the mean annual discharge of the two periods for the four rivers.

3.3.4 Baseflow separation and low flow analysis

The baseflows for Domasi, Likangala, Mulunguzi and Thondwe watersheds were separated from the daily flows using the recursive technique of Eckhardt (2005) which employs the use of a digital filter equation given by;

$$b_t = \frac{(1 - BFI_{max}) \times \alpha + b_{t-1} + (1-\alpha) \times BFI_{max} \times Q_t}{1 - \alpha \times BFI_{max}} \quad (3.1)$$

Where:

b_t = filtered baseflow at the t time step (m^3s^{-1})

b_{t-1} = filtered baseflow at time t-1 time step (m^3s^{-1})

BFI_{max} = maximum value of long term ratio of baseflow to streamflow

α = filter parameter

Q_t = total streamflow at the t time step (m^3s^{-1})

To achieve this computation the Web-based Hydrograph Analysis Tool (WHAT) system available at https://engineering.purdue.edu/mapserve/WHAT/ (accessed on 22nd February, 2017) was used. In addition to baseflows, low flows were also analysed using the annual minimum 7-day average flow ($Q_{7\text{-dmin}}$). The $Q_{7\text{-dmin}}$ was determined by isolating the lowest average flow of 7 consecutive days from each year analysed in this study. Time series plots of the baseflows and the $Q_{7\text{-dmin}}$ flows from 1970 to 1999 were produced for each river.

3.3.5 Hydroclimatological trends

Trend tests were done on rainfall, annual streamflow, baseflow and air temperature data. The Mann-Kendall (MK) non parametric test was used at a level of significance of 0.05 (α = 0.05). The annual rainfall (mm), annual average streamflow (m^3s^{-1}), baseflow (m^3s^{-1}) and mean monthly temperature (°C) within the Chilwa Basin were tested for trends. Equations 2.2 to 2.7 were used to establish if there was a trend in each data record. The rejection criterion for the null hypothesis was applicable when p-value was less than the level of significance ($p < \alpha = 0.05$).

3.3.6 Computation of probability of exceedance

The probability of exceedance was calculated for the daily rainfall and daily streamflow for the periods from 1970 to 1984 and 1985 to 1999 using the FDC 2.1 HydroOffice program. The streamflow data was formatted to text file format acceptable by the program. Long term exceedance probability for each period was calculated as percentiles at an interval of 0.5. Flow duration curves were then plotted as log-log plots for the two periods on the same axis. This enabled understanding of runoff characteristics exhibited between the two periods for each watershed.

3.4 Quantifying land use change impact on streamflow

The ArcSWAT 2012 was downloaded and installed as an extension of ArcGIS 10.2 to model streamflow. For the calibration of the model, the SWAT- Calibration and Uncertainty Program (SWAT-CUP 2012) was also downloaded and installed as a stand-alone program and was linked to ArcSWAT project through the TxtInOut folder.

3.4.1 SWAT model input data

The SWAT model requires geographic and climatic data as input. The specific datasets include a Digital Elevation model (DEM), soil map, land use maps, daily precipitation and daily maximum and minimum air temperature data. In this study, a DEM of 30m spatial resolution downloaded from http://www.earthexplorer.usgs.gov was used. In addition, the FAO-UNESCO soil map which is the Digital Soil Map of the World (DSMW) was downloaded in ESRI shapefile format from the FAO GeoNetwork website - www.fao.org/geonetwork. The DSMW was at a scale of 1:5,000,000 covering the entire Africa. The land use maps for 1973 and 1994 as described in section 3.2 were obtained and used in the modelling. The daily rainfall, daily temperature and daily streamflow dataset as described in section 3.3 were also used in the modelling.

3.4.2 Data preparation

The DEM and soil map were masked and clipped respectively in ArcMap to the size covering the whole Lake Chilwa Basin. Thereafter, the DEM, soil map and the land use maps for 1973 and 1994 were all projected to UTM (WGS 84 - Zone 36S). The UTM projection is recommended for map inputs into the SWAT model. The soil map was later converted from shapefile to raster (.tiff) format. The grid values on the maps and their corresponding land use and soil type (for the soil map) were identified.

The grid information was later used to create the land use and soil lookup tables that were later used in the ArcSWAT model. Climatic data in form of daily rainfall (mm) and daily maximum and minimum air temperature (°C) were converted from excel to text file (.txt) formats readable by ArcSWAT model. Due to data limitations in this study therefore, the other required unavailable data such as relative humidity, solar radiation and wind speed were generated by the SWAT model using the weather generator database of the model.

3.4.3 SWAT model run

A new SWAT project was created in ArcSWAT and its security settings changed to full control. Thereafter, the prepared DEM as described in section 3.4.2 was imported into the project. Flow accumulation, flow direction and stream networks were then processed. The watershed was then delineated after selecting the outlet point of the intended stream. In this study, Thondwe watershed was selected due to the availability of necessary weather data (daily rainfall and daily air temperature) for the SWAT simulations. Topographic output report was eventually produced, showing Thondwe watershed as having a maximum elevation of 1360m above mean sea level (a.m.s.l) and a minimum of 660m a.m.s.l. A total of 9 sub basins were obtained after delineation as shown in Figure 3.2.

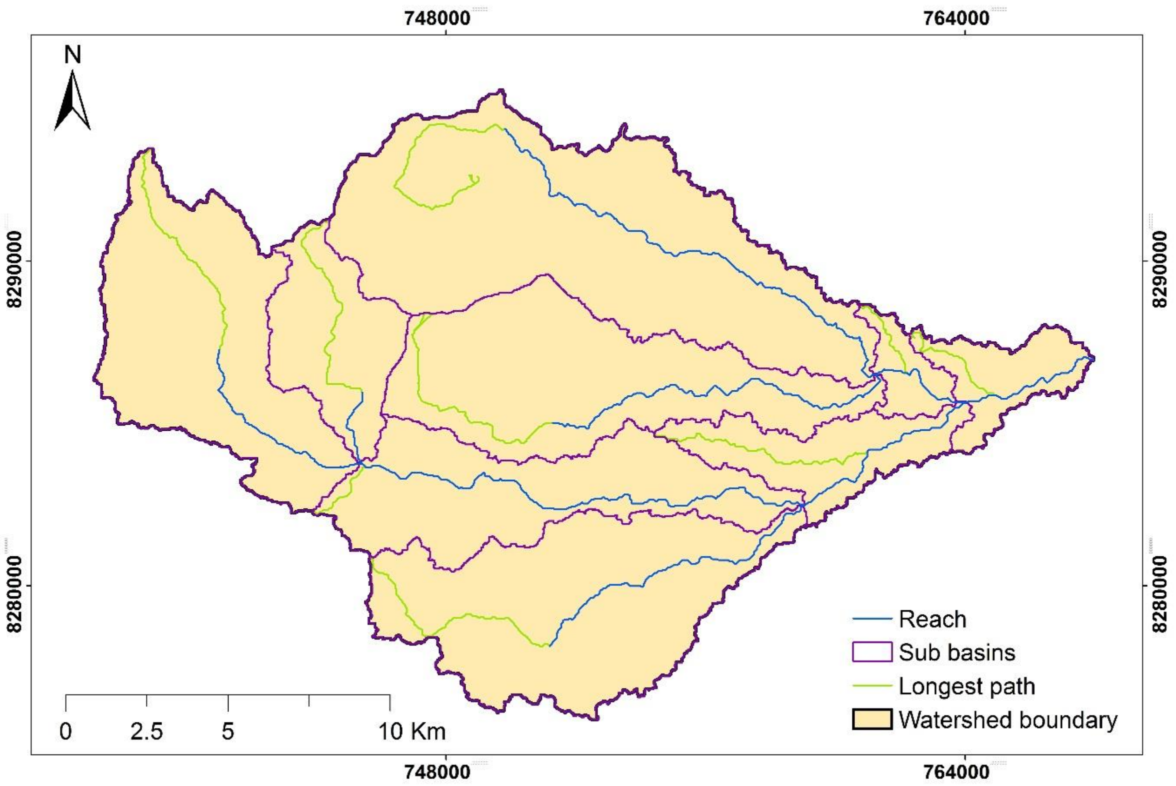

Figure 3.2: Delineated map of Thondwe watershed

After watershed delineation, the hydrological response unit (HRU) analysis was done to establish areas of similar land use, soil type and slope on the map. The land use map was therefore imported into the SWAT project and reclassified into SWAT recognised classes. The land use look-up tables as presented in the Appendices D10 and D11 were used as the link between the map grid values (for the 1973 and 1994 land use maps, respectively) and the SWAT land use classes in the database.

The FAO soil map was later imported into the project. Using the soils look-up table given in Appendix D12, the soils map was thereafter reclassified linking it with the SWAT database. Prior to importing the soil map however, modification was done to the SWAT *usersoil* database by adding the MWSWAT 2012 soils database copied from the database of MapWindow program, enabling compatibility of FAO soils with the SWAT model. Because of the small scale (1:5,000,000) for the soil map used, the entire Thondwe watershed was represented as having two soil types; the I - Bc - c (Lithosols) and the Ne54 - 2/3b (Eutric Nitosols) as shown in Figure 3.3. Based on the textural names provided in the MWSWAT database, the two soils are both clay loam with the Eutric Nitosols having slightly less clay content compared to the Lithosols.

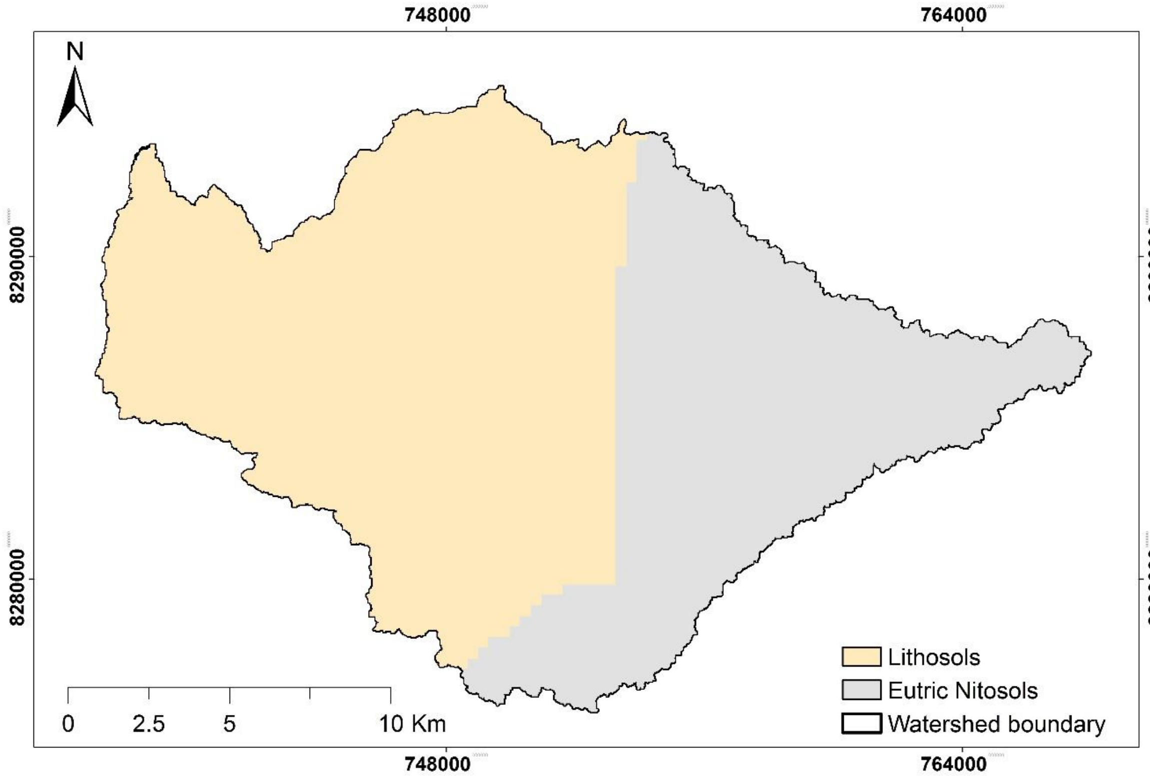

Figure 3.3: Soil map (FAO-DSMW) of Thondwe watershed

Land slopes were later classified into five classes of 0 to 10%, 10% to 20%, 20% to 30%, 30% to 50% and >50% as shown in Figure 3.4. An overlay of land use, soil type and slope was eventually done and the hydrologic response units (HRUs) created as shown in Appendix C7. The final HRU report was finally produced showing a total number of HRUs created for each land use map. A total of 191 HRUs were created with the 1973 land use map while 144 HRUs were created with the 1994 land use map.

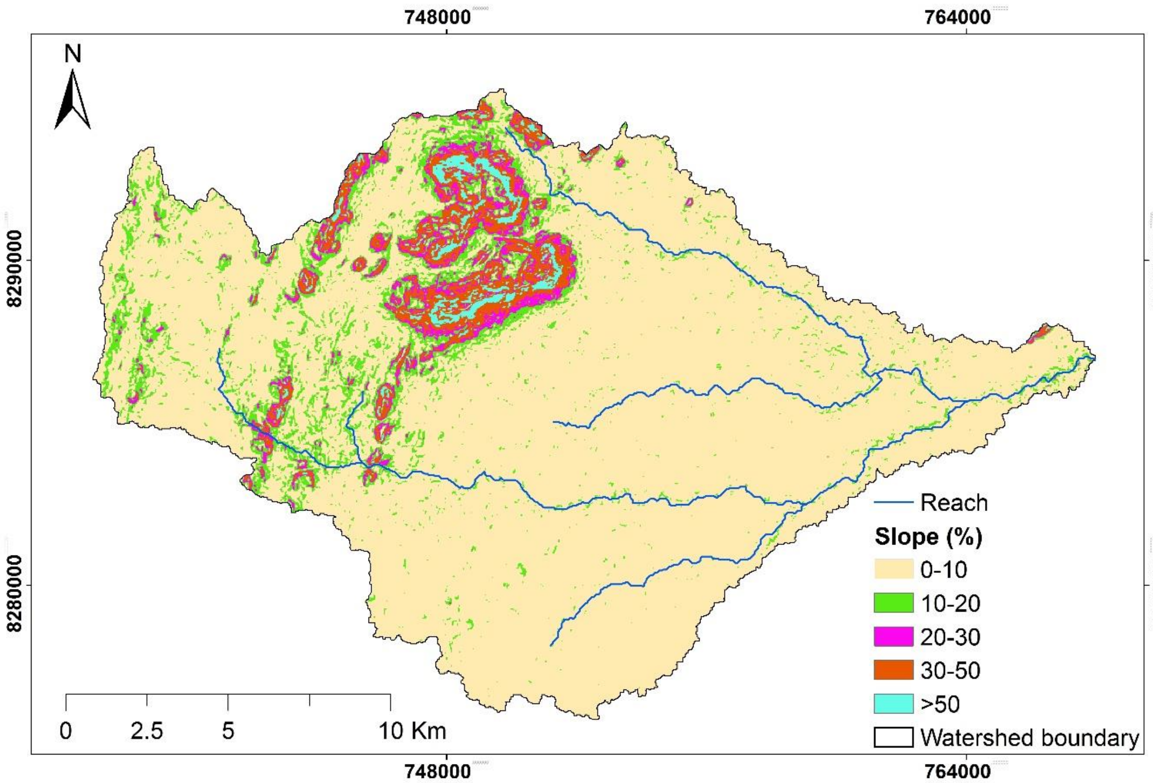

Figure 3.4: Land slope classification map of Thondwe watershed

Since the only available weather data were the daily rainfall and the daily maximum and minimum air temperature, these datasets were used as input into the model as text files. The model was allowed to simulate relative humidity, solar radiation and wind speed from SWAT weather generator (WGEN). The SCS curve number method (USDA-SCS, 1972) which uses daily rainfall to estimate surface runoff was used in the simulations.

3.4.4 Sensitivity analysis, calibration and validation

In this study, the global sensitivity analysis technique was performed to identify parameters with much influence to flow simulation. The Sequential Uncertainty Fitting version 2 (SUFI2) in SWAT- CUP was used for sensitivity analysis, calibration and validation. During the sensitivity analysis, ten objective functions in the SUFI2 were tried one after another to check their effect on calibration results. Eventually, the modified Nash-Sutcliffe efficiency factor (MNS) was used raised to power one (p = 1). The MNS with p = 1 has an ability to reduce overestimation of peaks which made it suitable for its application in this study. Table 3.1 shows the flow parameters that were considered in the flow sensitivity analysis and their description.

Table 3.1: **List of parameters used in flow sensitivity analysis**

S/No	Name	Description	Range
1	ALPHA_BF	Baseflow alpha factor	0 – 1
2	BIOMIX	Biological mix efficiency	0 – 1
3	CANMX	Maximum canopy storage	0 – 100
4	CH_K2	Effective hydraulic conductivity in the main channel alluvium	0 – 500
5	CH_N2	Manning's "n" value for the main channel	-0.01 – 0.3
6	CN2	SCS runoff curve number	35 – 98
7	EPCO	Plant compensation factor	0 – 1
8	ESCO	Soil evaporation compensation factor	0 – 1
9	GW_DELAY	Groundwater delay	30 – 450
10	GW_REVAP	Groundwater revap coefficient	0 – 1
11	OV_N	Manning's "n" value for overland flow	0 – 30
12	RCHRG_DP	Deep aquifer percolation fraction	0 – 1
13	SOL_AWC	Available water content of soil	0 – 1
14	SOL_BD	Moist bulk density	0 – 1
15	SURLAG	Surface runoff lag time	0 – 24

From the sensitivity analysis, the five most sensitive parameters to flow simulation were used in the calibration of the model. The other ten parameters were assumed not to have much influence on flow simulation and were therefore not included. Calibration was done with up to 500 simulations performed as the recommended minimum number for SWAT-CUP calibration when determining best parameter values. At 500 simulations, SWAT-CUP almost reaches stability and there is an insignificant change in parameter values with more simulations performed (Abbaspour, 2012). The five year periods from 1983 to 1987 and 1988 to 1992 were used for calibration and validation, respectively. The observed monthly flow data was used in the calibration and validation.

The performance of the model was later assessed using the Nash-Sutcliffe (NS) (Equation 2.12), the coefficient of determination (R^2) (Equation 2.13), percent bias (PBIAS) (Equation 2.14) and the root mean square error-observations standard deviation ratio (RSR) (Equation 2.15). Thereafter, best fit parameter values obtained after the calibration were used in the scenario runs for the estimation of climate variability and land use change effects on runoff for the study period of 1970 to 1999.

3.4.5 Quantifying the impact of climate variability and land use change on streamflow

In this study, four hypothetical scenarios (S1, S2, S3 and S4) as described in Li *et al.* (2009) were used to assess the impact of climate and land use change on streamflow. Table 3.2 shows the setup combinations of the four simulation scenarios. The simulated results rather than the observed data were used to compare hydrological effects of land use change and climate variation on flow in the Thondwe watershed to give an example representation of a system, so as to understand the hydrological processes of Lake Chilwa Basin.

Table 3.2: Scenario setup for the climate variability and land use change simulations

Scenario	Land use map	Climatic data
S1	1973	1970 - 1984
S2	1994	1970 - 1984
S3	1973	1985 - 1999
S4	1994	1985 - 1999

In the first scenario (S1), the 1973 land use map was used to simulate streamflow for the 1970 to 1984 period. As for the second scenario (S2), the 1994 land use map was used instead to simulate streamflow for the same period of 1970 to 1984, all other factors such as climatic data and parameter values were held constant as in S1. The simulated results from S2 were compared with those of S1 to estimate the impact of land use change. The effect of climate variability was assessed in the third scenario (S3), in which the 1985 to 1999 climatic data was used while maintaining the 1973 land use. Comparison of simulated runoff from S3 and S1 was made to determine the impact of climate variability. Lastly, the 1994 land use map and the 1985 to 1999 climatic data were used to simulate runoff in scenario four (S4); whose results were compared with S1 results to determine the combined effect of land use change and climate variability.

3.4.6 Impact on evapotranspiration and soil water

The impact of climate variability and land use change on evapotranspiration and soil water was also estimated using SWAT simulations. The simulated average annual soil water (SW) and annual evapotranspiration (ET) from the four scenarios (S1, S2, S3 and S4) as shown in Table 3.2 were compared. In this study, the potential evapotranspiration (PET) and actual evapotranspiration (ET) were estimated using the Hargreaves method as it requires less data input compared to other methods such as the Penman-Monteith. The Hargreaves equation

(Hargreaves and Allen, 2003) for the estimation of potential evapotranspiration (PET) is given by:

$$ET_0 = 0.0023Ra(T_{\max} - T_{\min})^{0.5}\left[\frac{T_{\max} + T_{\min}}{2} + 17.8\right] \quad (3.2)$$

Where:

ET_o = Reference evapotranspiration (*mm day*$^{-1}$)

Ra = Extraterrestrial radiation (*MJ m*$^{-2}$ *day*$^{-1}$)

T_{max} = Maximum air temperature (°*C*)

T_{min} = Minimum air temperature (°*C*)

The actual evapotranspiration (ET) in the SWAT model is estimated by taking into consideration the influence of factors such as ground cover and canopy properties (Jovanovic and Israel, 2012), given by:

$$ET = k_c ET_o \quad (3.3)$$

Where: k_c = coefficient representing influence of crop on evapotranspiration

The estimation of the annual soil water (SW) by SWAT model uses the water balance formulation as described in (Neitsch *et al.* (2005) given by:

$$SW_t = SW_0 + \sum_{i=1}^{t}(R_{day} - Q_{surf} - E_a - w_{seep} - Q_{gw}) \quad (3.3)$$

Where:

SW_t = the final soil water content (*mm*)

SW_0 = the initial soil water content on day *i* (*mm*)

t = time (*days*)

R_{day} = amount of precipitation on day *i* (*mm*)

Q_{surf} = amount of surface runoff on day *i* (*mm*)

E_a = amount of evapotranspiration on day *i* (*mm*)

W_{seep} = amount of water entering the vadose zone from the profile on day *i* (*mm*)

Q_{gw} = amount of return flow on day *i* (*mm*)

CHAPTER FOUR

RESULTS AND DISCUSSIONS

4.1 Changes in land use

4.1.1 Land use change at basin level

Figure 4.1 shows land use thematic maps for Lake Chilwa Basin produced after the supervised image classification. The areas in square kilometers (km^2) and proportion cover (%) of each land use class for the analysed years of 1973, 1994 and 2013 are presented in Table 4.1.

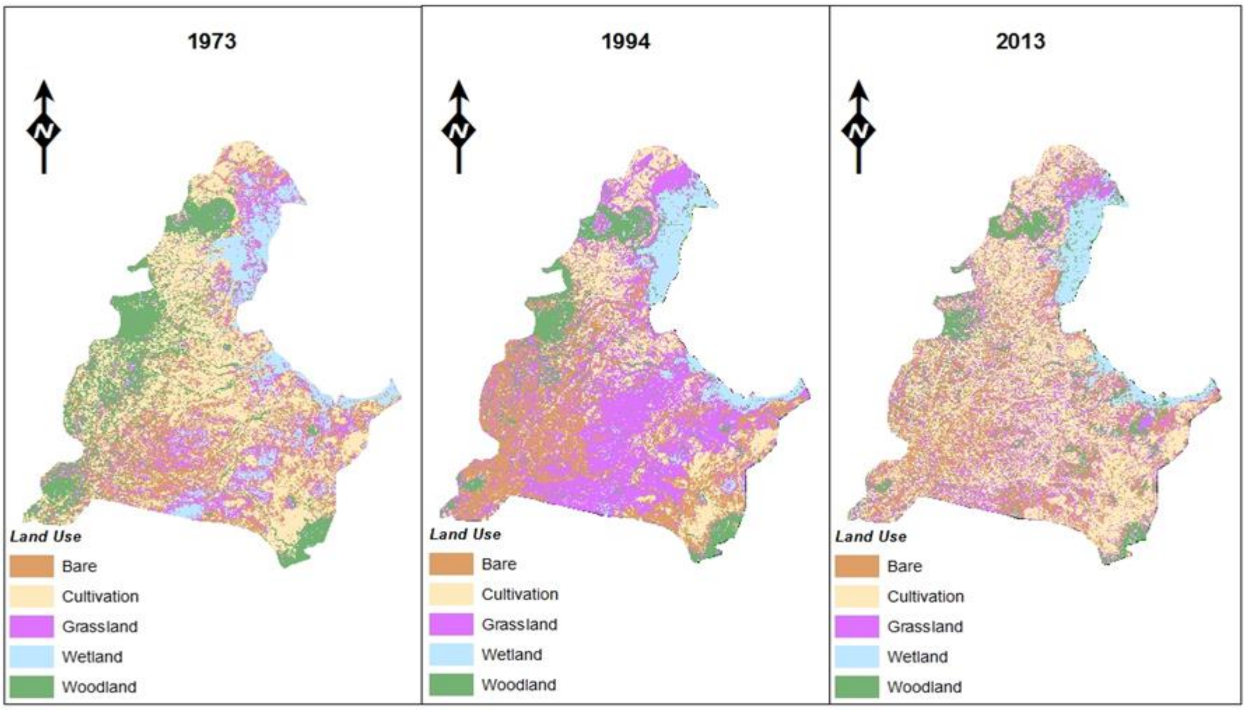

Figure 4.1: Land use thematic maps for Lake Chilwa Basin

Table 4.1: Land use area and percent cover for Lake Chilwa Basin

		Bare land	Cultivation	Grassland	Wetland	Woodland
1973	Area (km^2)	994.7	1084.5	411.2	755.8	472.8
	Area (%)	26.7	29.2	11.1	18.9	14.1
1994	Area (km^2)	921.6	1541.6	663.9	335.5	256.3
	Area (%)	24.7	41.5	17.9	9.0	6.9
2013	Area (km^2)	790.0	1752.8	695.5	247.9	232.8
	Area (%)	21.2	47.1	18.7	6.7	6.3

From the image analysis results in Figure 4.1, five (5) major classes of land use or cover (LULC) were obtained in the basin namely; bare land, cultivation, grassland, wetland and woodland. Land use areas as retrieved from the 1973, 1994 and 2013 images using remote sensing techniques reveal changes in land use proportions in the basin. From the results in Table 4.1, it is evident that the proportion of cultivated land increased at basin level from 1084.5 km^2 in 1973 to 1541.6 km^2 in 1994 and 1752.8 km^2 in 2013. This represents 42% increase between 1973 and 1994 and 13% increase between 1994 and 2013. Mindle *et al.* (2001) suggested that agricultural statistics in Malawi increased substantially under maize and tobacco cultivation between 1970 and 1994.

Further analysis of the LULC change results for the basin shows that as cultivated land increased between 1973 and 2013, the areas under forest, wetland and bare land subsequently declined at basin level from 14.1% to 6.3%, 18.9% to 6.7%, and 26.7% to 21.2% respectively. The reduction in wetland within the Lake Chilwa Basin, according to Kafumbata *et al*. (2014), was largely due to an increase in subsistence agriculture. Foli and Makungwa (2011) also observed that expansion of smallholder farming units in Malawi, generally led to deforestation. In most cases, declining forests and increasing agricultural land are predictors of a degraded state of the environment (Allan, 2004).

4.1.2 Land use change within watersheds

Figures 4.2 - 4.5 show results of land use change for Domasi, Likangala, Mulunguzi and Thondwe watersheds, respectively. Tabulated results are presented in Appendix D1 and the thematic maps for the land use change are presented in Appendices C3 to C6.

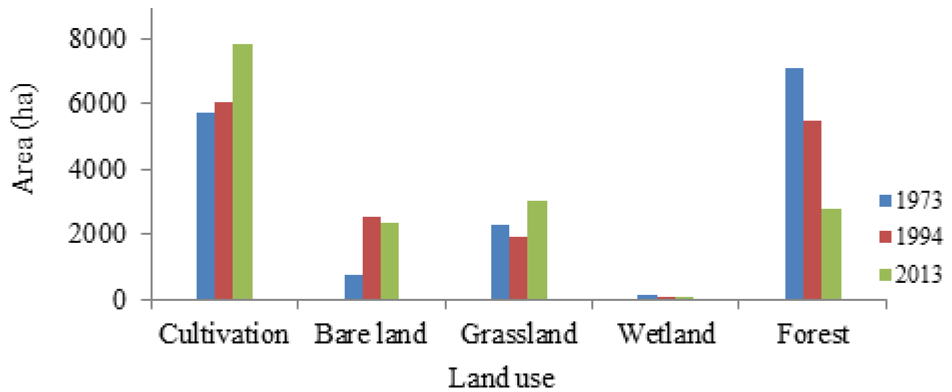

Figure 4.2: Land use change in Domasi Watershed (1973 to 2013)

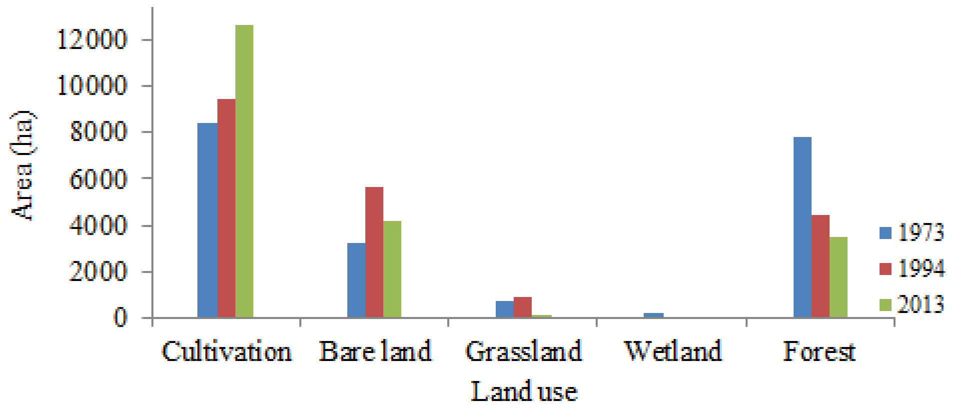

Figure 4.3: Land use change in Likangala Watershed for the period 1973 to 2013

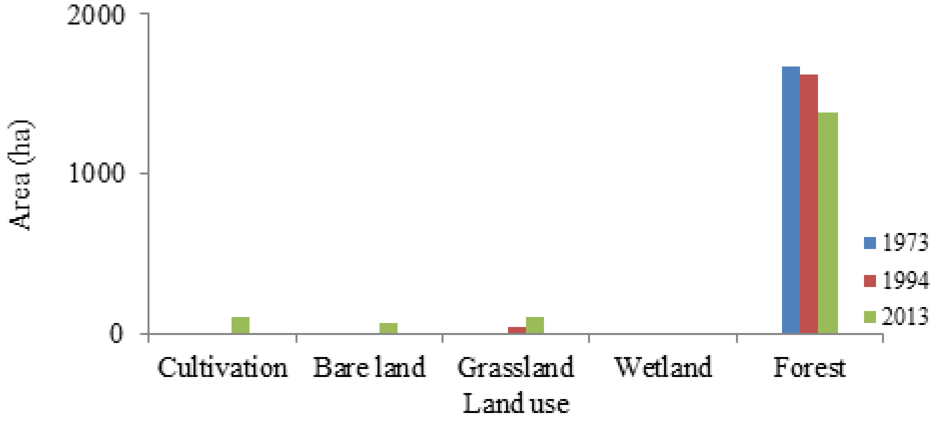

Figure 4.4: Land use change in Mulunguzi Watershed for the period 1973 to 2013

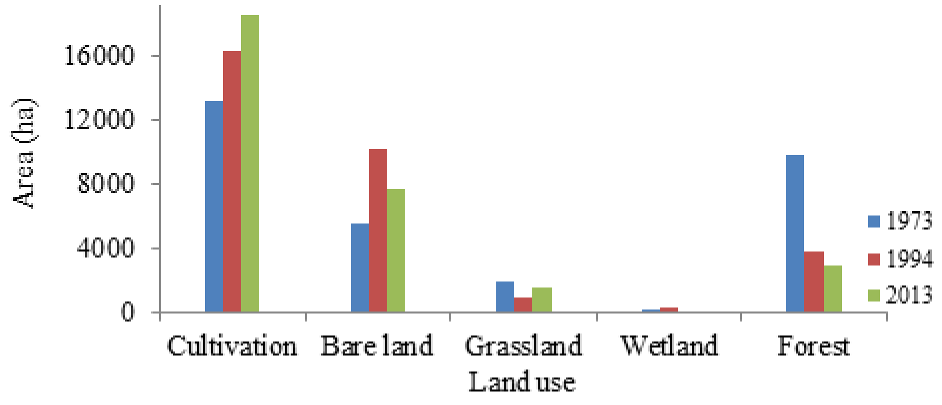

.

Figure 4.5: Land use change in Thondwe Watershed for the period 1973 to 2013

As shown in Figures 4.2 - 4.5, there was a general increase in cultivated land in the watersheds of Domasi, Likangala and Thondwe. Bare land also increased in Domasi, Likangala and Thondwe watersheds between 1973 and 1994 due to accelerated deforestation for agricultural expansion. There was however a decline in bare land in Domasi, Likangala and Thondwe between 1994 and 2013 as the marginal bare land was converted to cultivation.

Mulunguzi watershed as shown in Figure 4.4 however had a unique LULC with highest forest proportion of 99.73% in 1973 and 96.9% in 1994. As shown in Figure 4.4, there was insignificant cultivation in Mulunguzi watershed between 1973 and 1994. As forest vegetation decreased, there was an increase of grassland area in the Mulunguzi watershed. From the results, it is also shown that the wetland area generally reduced in all the four watersheds between 1973 and 2013. The results however show no clear trend in grassland areas for the different watersheds.

4.2 Hydroclimatological changes

4.2.1 Rainfall amount

Table 4.2 shows summary t-test results on rainfall amount from 1970 to 1984 and 1985 to 1999. Full t-test results for each gauge station are presented in Appendices D2 to D5.

Table 4.2: Student's t-test results for annual rainfall (1970 to 1984 and 1985 to 1999)

Station	$t_{\text{Calculated}; \alpha = 0.05}$	$t_{\text{Critical (two tailed)}}$
Chancellor College	0.0016	2.0484
Domasi	0.8924	2.0484
Makoka	1.1575	2.0484
Zomba Plateau	1.3593	2.0484

From the results in Table 4.2, it is evident that there was no significant difference in the annual rainfall from 1970 to 1984 and 1985 and 1999 for the analysed stations of Chancellor College, Domasi, Makoka and Zomba Plateau at 95% level of confidence. Further analysis was therefore done on rainfall to check for seasonal rainfall patterns and trends.

4.2.2 Rainfall patterns

Figures 4.6 - 4.9 present results of rainfall pattern analysis for Chancellor College, Domasi, Makoka and Zomba Plateau rainfall stations within the Lake Chilwa Basin.

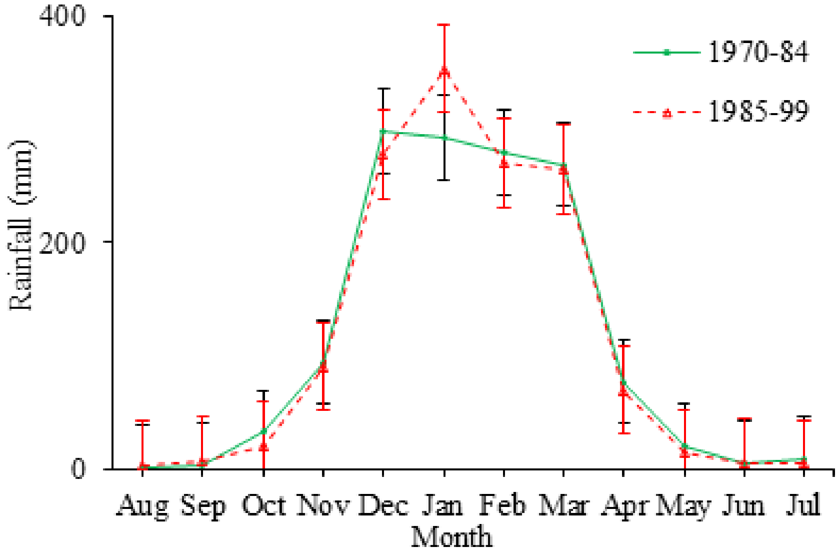

Figure 4.6: Long-term mean monthly rainfall patterns for the period before land use changes (1970 to 1984) and post-change period 1985 to 1999) at Chancellor College Station. The error bars indicate the standard error for each month

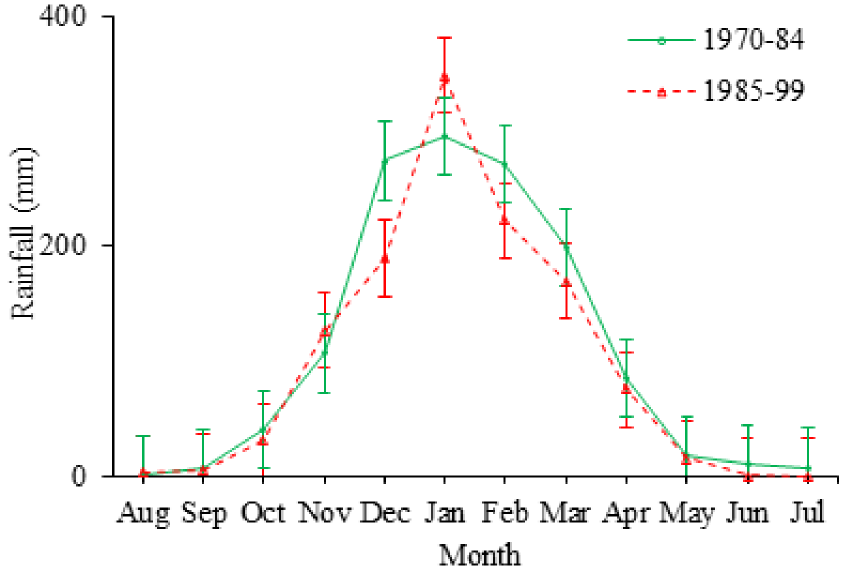

Figure 4.7: Long-term mean monthly rainfall patterns for the period before land use changes (1970 to 1984) and post-change period (1985 to 1999) at Domasi Station. The error bars indicate the standard error for each month

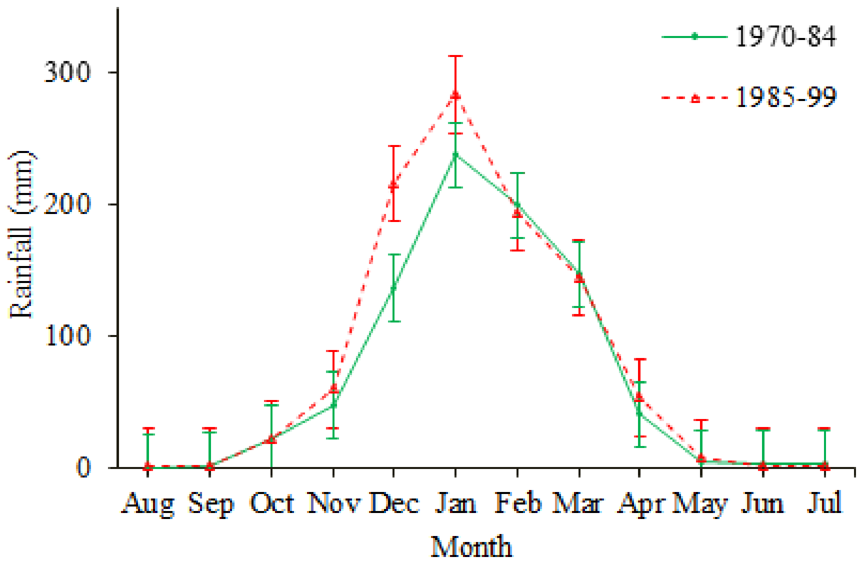

Figure 4.8: Long-term mean monthly rainfall patterns for the period before land use changes (1970 to 1984) and post-change period (1985 to 1999) at Makoka Station. The error bars indicate the standard error for each month

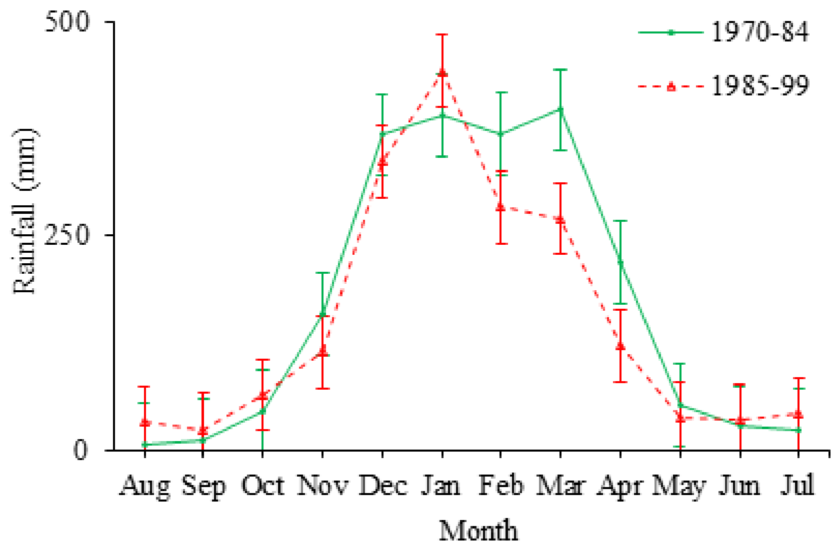

Figure 4.9: Long-term mean monthly rainfall patterns for the period before land use changes (1970 to 1984) and post-change period 1985 to 1999) at Zomba Plateau Station. The error bars indicate the standard error for each month

From the results in Figures 4.6 - 4.9, it is apparent that there has been a seasonal change or shift in rainfall pattern over the 1970 to 1999 period. For instance, the rainfall patterns at Chancellor College, Domasi and Zomba Plateau Stations show a delayed onset of rainfall season from October towards November in the latter period of 1985 to 1999. Such delay in rainfall onset however was not observed at Makoka Station (Figure 4.8). In addition, there was generally a quicker rainfall cessation tendency observed for the 1985 to 1999 period compared to the 1970 to 1999 period. Recent reports by the IPCC (2007) project that rainfall will decrease in the southern Africa region by the year 2050.

4.2.3 Mean annual streamflow

Table 4.3 shows t-test summary results on the mean annual streamflow for Domasi, Likangala, Mulunguzi and Thondwe Rivers for the periods 1970 to 1984 and 1985 to 1999. For detailed t-test results refer to Tables D6 to D9.

Table 4.3: Summary t-test results for the average annual discharge

River	$t_{\text{Calculated}, \alpha = 0.05}$	$t_{\text{Critical (two tailed)}}$
Domasi	0.5193	2.0484
Likangala	0.5298	2.0484
Mulunguzi	0.6651	2.0484
Thondwe	1.4656	2.0484

Results of t-test as shown in Table 4.3 indicate that there was no significant difference in the mean annual discharge for the two periods at a level of significance of 0.05 for all the watersheds. These results are in direct relationship with t-test results on annual rainfall that did not detect any significant difference for the two periods at a significance level of 0.05. Rejection criterion for the null hypothesis stating that there was no significant difference in streamflow between the periods of 1970 to 1984 and 1985 to 1999 was if t-stat was greater than t-critical. The results show therefore that the mean annual discharges have fairly been constant and match observations in rainfall results reported in Section 4.2.1.

4.2.4 Annual rainfall and mean annual flow trends

Figures 4.10 - 4.13 show time series plots of rainfall and discharge for Domasi, Likangala, Mulunguzi and Thondwe watersheds. The Mann-Kendall trend test results for the annual rainfall and average annual discharge are presented in Tables 4.4 and 4.5.

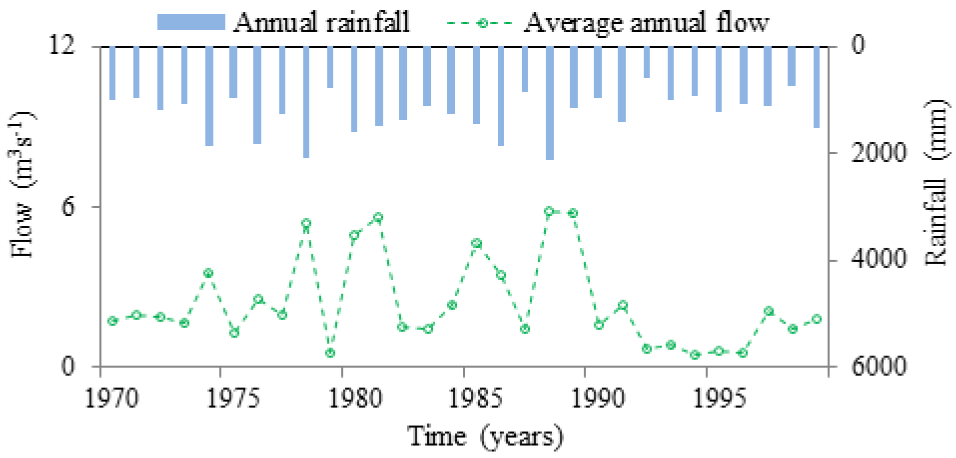

Figure 4.10: Annual rainfall and river flow time series for Domasi watershed

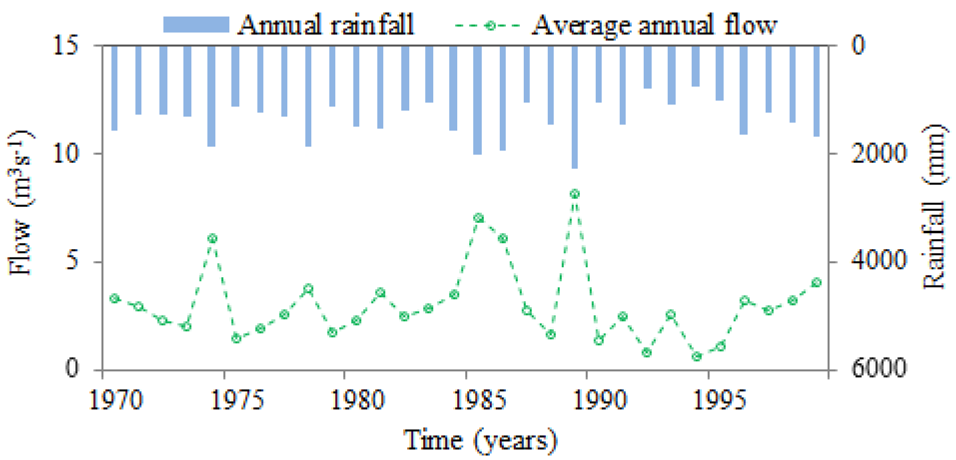

Figure 4.11: Annual rainfall and river flow time series for Likangala watershed

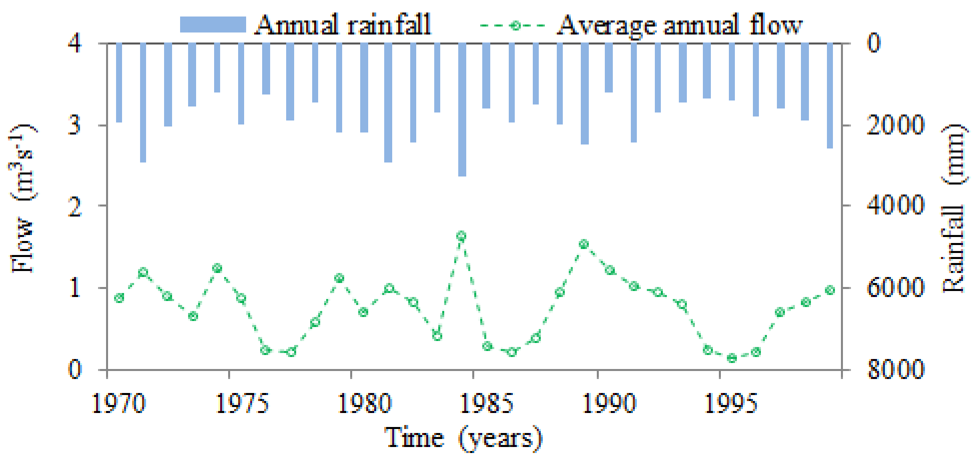

Figure 4.12: Annual rainfall and river flow time series for Mulunguzi watershed

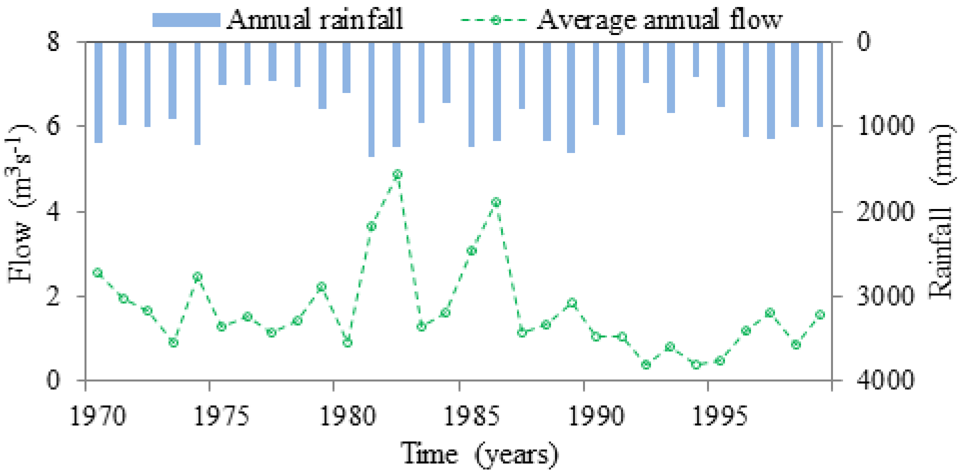

Figure 4.13: Annual rainfall and river flow time series for Thondwe watershed

Table 4.4: Mann-Kendall trend test results for annual rainfall (1970-1999)

Rainfall station	S	Var (S)	$P_{(0.05)}$	Sen's slope
Chancellor College	-44	3140.67	0.443	-0.012
Domasi College	-29	3141.00	0.617	-0.031
Makoka Research	-11	3141.67	0.858	-0.001
Zomba Plateau	22	3140.67	0.708	0.003

As presented in Table 4.4, the monotonic trends of annual rainfall show no significant ($p = 0.05$) increasing or decreasing trend in all the stations. Based on the Sen's slope however, the annual rainfall for Chancellor College, Domasi and Makoka with the exception of Zomba Plateau showed some decreasing tendency which was however not significant at $\alpha = 0.05$. Table 4.5 shows the MK trend test results for Domasi, Likangala, Mulunguzi and Thondwe watersheds.

Table 4.5: Mann-Kendall trend test results for the average annual discharge (1970 to 1999)

River	S	Var (S)	$P_{(0.05)}$	Sen's slope
Domasi	-75.0	3141.667	0.197	-0.019
Likangala	-9.0	3141.667	0.897	-0.009
Mulunguzi	-49.0	3141.667	0.392	-0.005
Thondwe	-29.0	3141.667	0.250	-0.018

From the results in Table 4.5, no significant trend ($p = 0.05$) was detected in the mean annual streamflow for all watersheds. The Sen's slope shows a negative and therefore decreasing tendency for all the four river watersheds although not significant at $\alpha = 0.05$. The decreasing tendency could largely be linked to a similar tendency in the rainfall trend. No significant trend was however detected in both the annual rainfall and the mean annual flows.

4.2.5 Trends in baseflow and low flows ($Q_{7\text{-dmin}}$) flow

Table 4.6 shows MK trend test results on baseflow for the Domasi, Likangala, Mulunguzi and Thondwe Rivers. The baseflow time series plots of the rivers are presented in Figures 4.14 - 4.17.

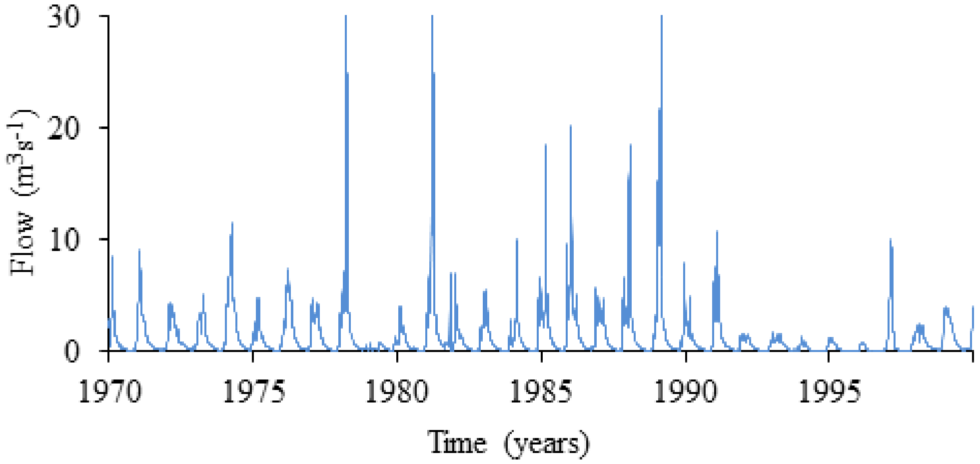

Figure 4.14: Baseflow time series for Domasi River (1970 to1999)

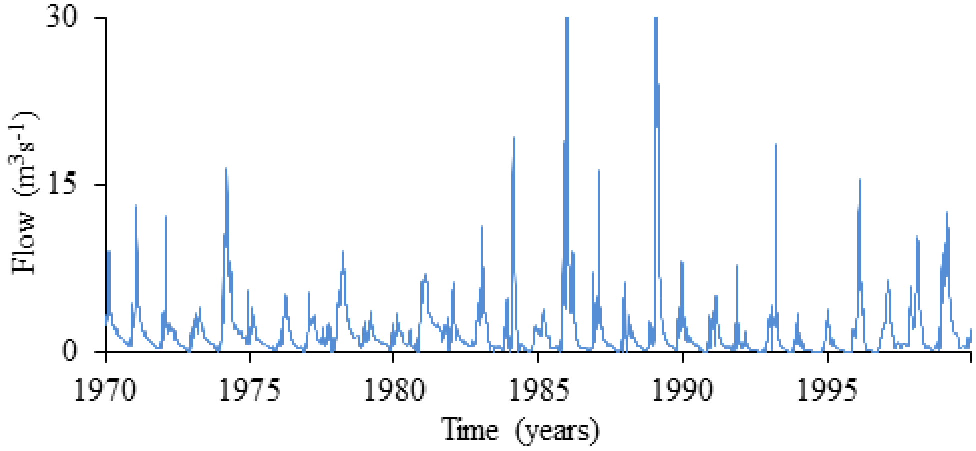

Figure 4.15: Baseflow time series for Likangala River (1970 to 1999)

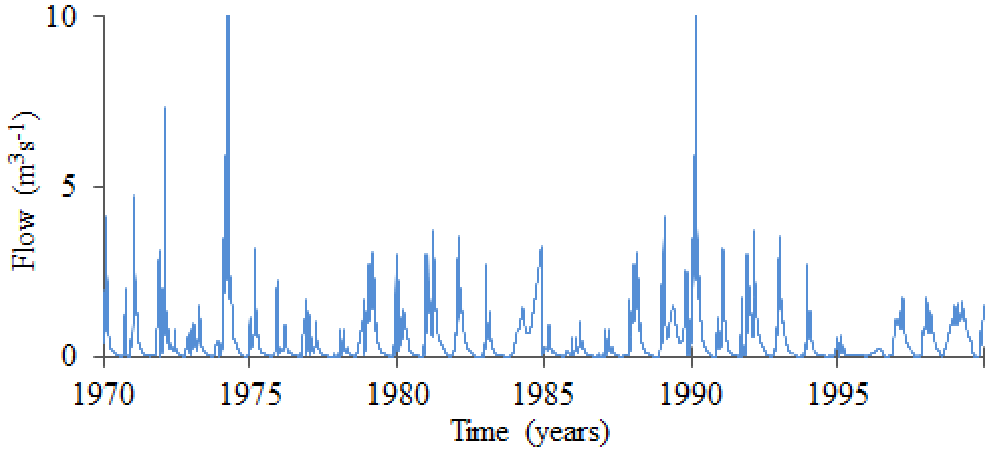

Figure 4.16: Baseflow time series for Mulunguzi River (1970 to 1999)

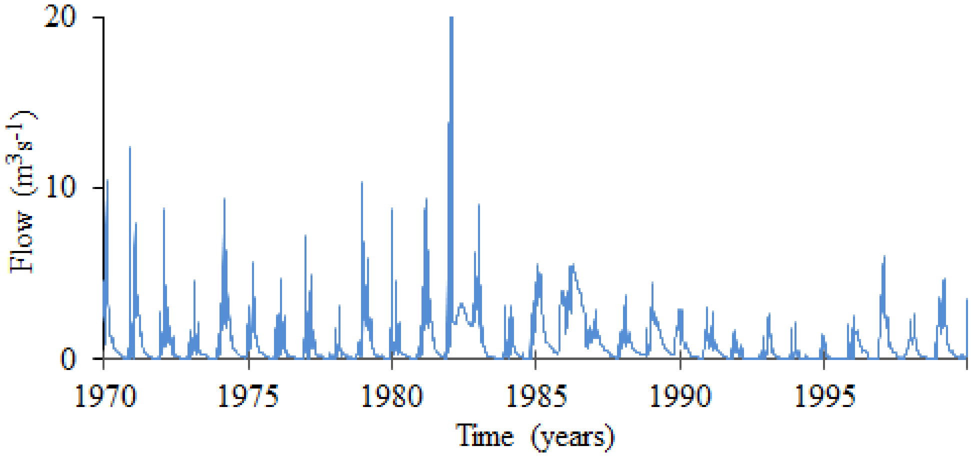

Figure 4.17: Baseflow time series for Thondwe River (1970 to 1999)

Table 4.6: Mann-Kendall trend test results for baseflows (1970 to 1999)

River	S	Var (S)	*P* (0.05)	Sen's slope
Domasi	-34770	1146645	< 0.0001**	-0.0132
Likangala	-33124	1146663	< 0.0001**	-0.0214
Mulunguzi	4731	1146166	< 0.0001**	0.0004
Thondwe	-15508	1146599	< 0.0001**	-0.0421

** Significant trend

The MK trend analysis for baseflows showed a significant ($p = 0.05$) decreasing trend for Domasi, Likangala and Thondwe Rivers. These watersheds were deforested as explained in Section 4.1.2. Similarly the 7-day minimum annual average flow (low flows) for the three deforested watersheds also showed significant declines as shown in Figures 4.18 to 4.20.

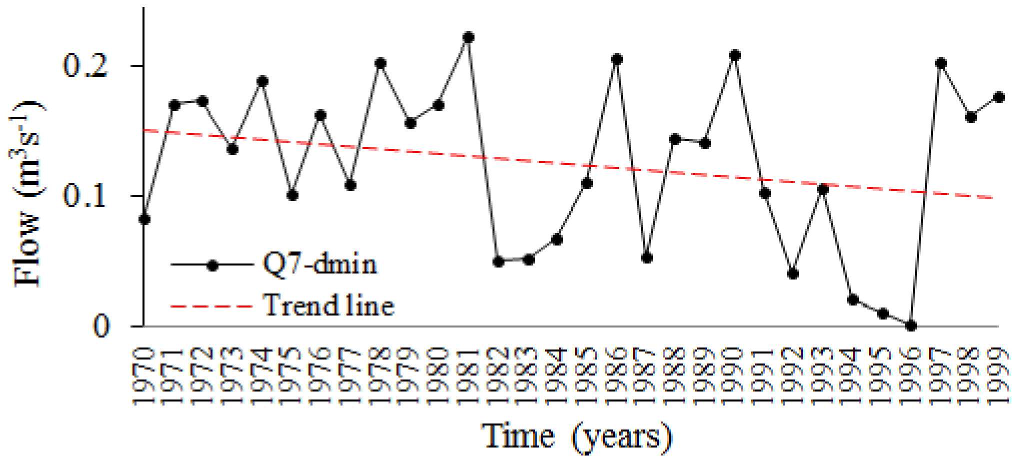

Figure 4.18: Low flow ($Q_{7\text{-dmin}}$) time series from 1970 to 1999 for Domasi Watershed

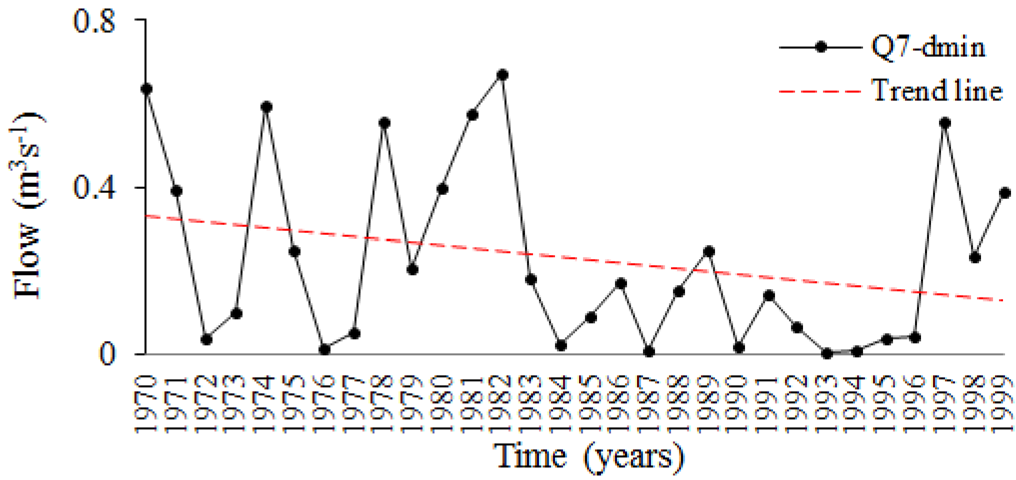

Figure 4.19: Low flow ($Q_{7\text{-dmin}}$) time series from 1970 to 1999 for Likangala Watershed

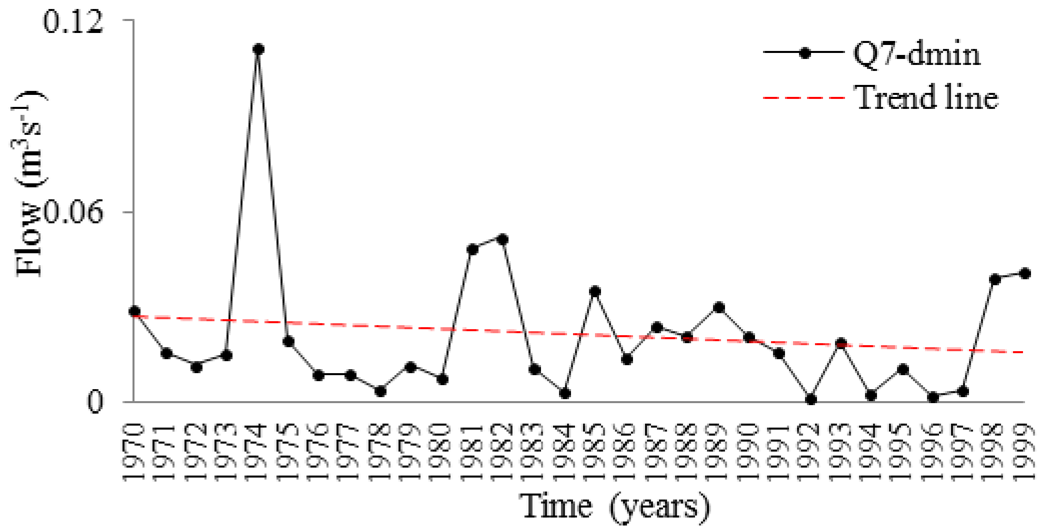

Figure 4.20: Low flow ($Q_{7\text{-dmin}}$) time series from 1970 to 1999 for Thondwe Watershed

The decline in baseflow and 7 day minimum annual average flow in these three watersheds was likely due to a more pronounced watershed response to rainfall, leading to a reduced groundwater recharge. Study by Bruijnzeel (2004) on the hydrological functions of tropical forests showed that forests generally enhance a complex intertwine of soils, roots and litter which acts as a "sponge" soaking up water during the rainy season releasing it evenly during the dry spell. Lal (1987) observed that as a result of deforestation, the "sponge effect" is often lost through the rapid oxidation of soil organic matter and compaction by raindrops and grazing among other factors, which tends to increase runoff and less seepage.

The declining baseflow in these three deforested watersheds of Domasi, Likangala and Thondwe may therefore be attributed to reduced groundwater recharge due to increase runoff as a result of deforestation. While the focus of this study was between 1970 and 1994, the 2013 Landsat image analysed in this study during ground-truthing shows further deforestation in these watersheds which implies continued decline in baseflows. Unlike in the deforested watersheds, baseflow for Mulunguzi watershed showed a significant (*p = 0.05*) increasing trend (Figure 4.16); attributed to a significant forest cover (explained in Section 4.1.2). The $Q_{7\text{-dmin}}$ also showed an increasing trend as shown in Figure 4.21.

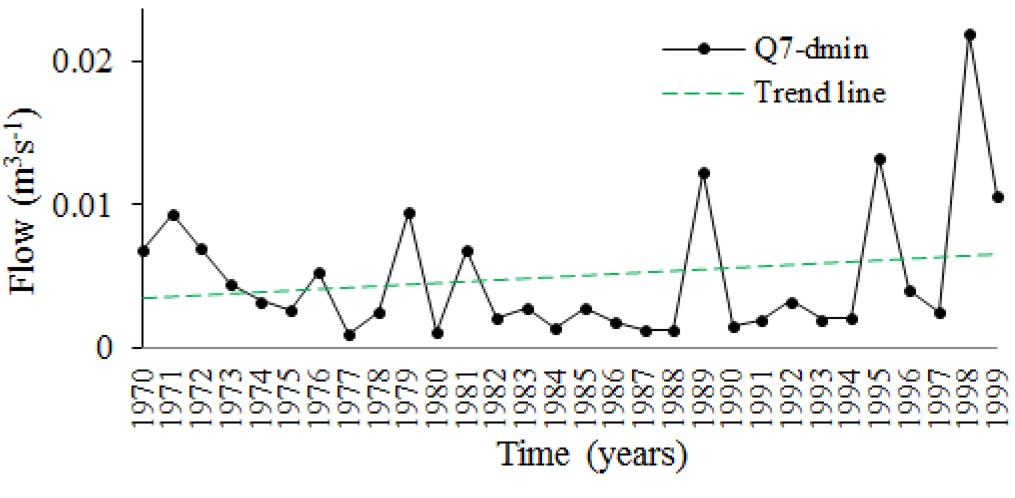

Figure 4.21: Low flow ($Q_{7\text{-dmin}}$) time series from 1970 to 1999 for Mulunguzi Watershed

Although there was a reduction in forest cover in the Mulunguzi watershed from 99.7% to 96.9% between 1973 and 1994, such forest reduction was largely replaced by grassland. Grasslands, just as forests also reduce overland flow and enhance groundwater recharge (Adams *et al.,* 2012). Kiersch (2000) noted that groundwater recharge contributes much to river flow during the dry season. Findings from separate studies by Mumeka (1986) and Jipp *et al.* (1998) showed that the conversion of tropical forests to grassland or pasture increases baseflows with up to 150 mm to 300 mm per year depending on rainfall amounts, due to less groundwater uptake by grasses compared to forests. This process seems to be the case for Mulunguzi which has experienced minor land use conversion from previously forested to grassland. The removal of few trees in Mulunguzi being replaced by grassland may have led to increased groundwater recharge and retention and increased release during the dry spells.

4.2.6 Temperature trends

Table 4.11 shows trend test results on the maximum and minimum temperatures for Makoka and Chancellor College stations. Due to data limitations, these stations were the only ones considered. The average annual maximum and minimum temperature time series plots for Chancellor College and Makoka stations are as shown in Figures 4.22 and 4.23.

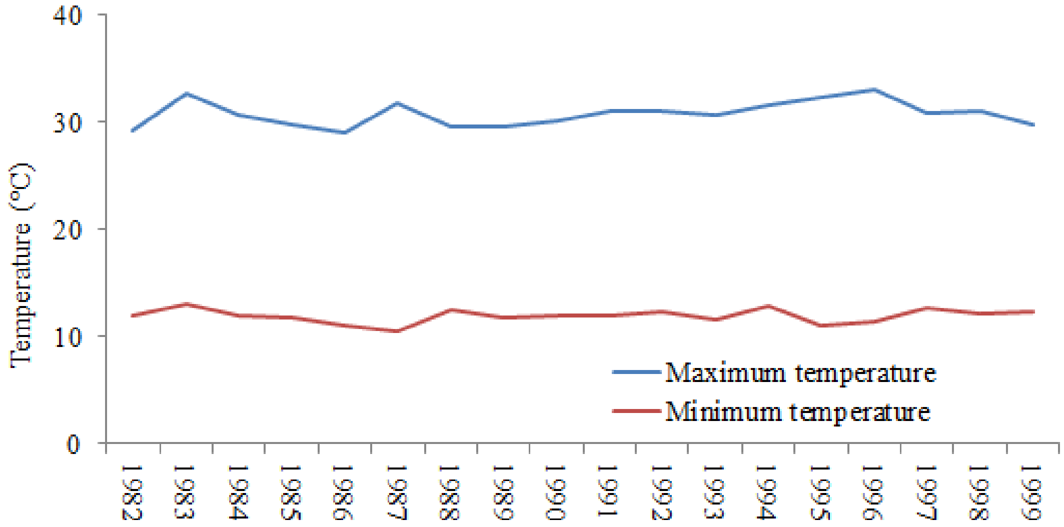

Figure 4.22: Temperature time series (max and min) for Chancellor College

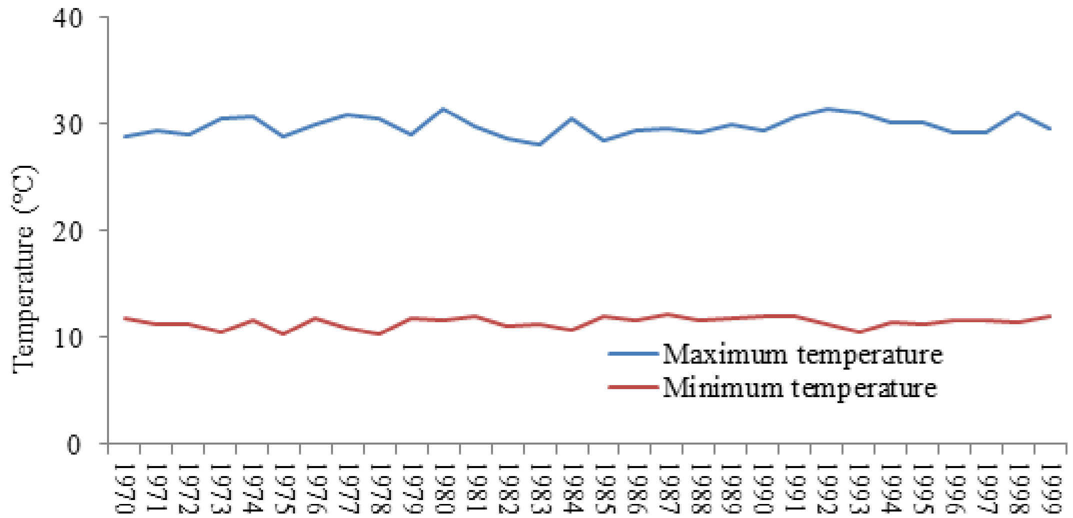

Figure 4.23: Temperature time series (max and min) for Makoka Station

Table 4.7: Mann Kendall trend test results for the average monthly temperatures

Station	S	Var (S)	P (0.05)	Sen's slope
Makoka (max)	968	37700	<0.0001	0.0263
Makoka (min)	510	37700	0.0090**	0.0122
Chancellor (max)	19	8297	0.843	0.0001
Chancellor (min)	146	8273	0.111	0.0003

** Significant trend

From the temperature trend test results in Table 4.7, the monthly maximum and minimum temperatures at Makoka showed a significantly (*p = 0.05*) increasing trend. Results for Chancellor College however did not show a significant trend. This could be because the trend test on temperature for Chancellor College considered a shorter period from 1982 to 1999 because of data limitations. The period tested for trends may influence trend results.

Bae *et al.* (2008) found out from their study that trend detection is often sensitive to dataset selected and period, indicating that different conclusions might be drawn with different dataset and period considered. From the results in Table 4.7, there was however a positive Sen's slope for both the maximum and minimum temperatures for Chancellor College, suggesting that temperatures tended to increase. The IPCC (2013) projections indicate that in the Southern Africa (Malawi inclusive); climate change will lead to increases in temperature by 4°C by the end of the century.

4.2.7 Exceedance probability of rainfall and streamflow

Figure 4.24 shows daily rainfall duration curves for Makoka station, chosen because its rainfall data was available as daily step, unlike the other stations whose datasets were available as monthly step. Figures 4.25 to 4.28 show daily flow duration curves (FDC) for Domasi, Likangala, Mulunguzi and Thondwe watersheds.

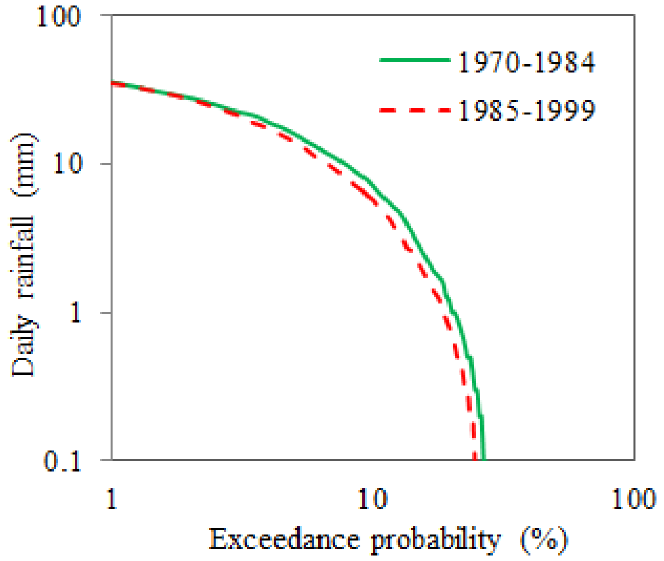

Figure 4.24: Daily rainfall duration curves for Makoka station (Thondwe watershed) for the pre- and post-land use change periods.

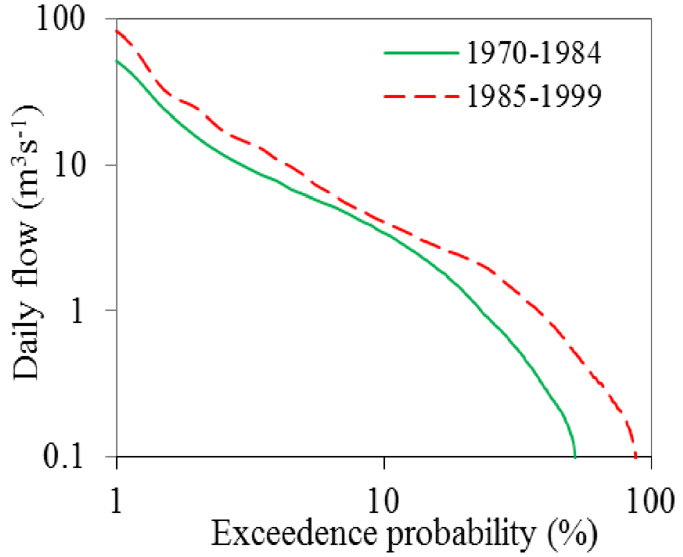

Figure 4.25: Daily flow duration curves before land use change (1970 to 1984) and after land use change (1985 to 1999) for Domasi River

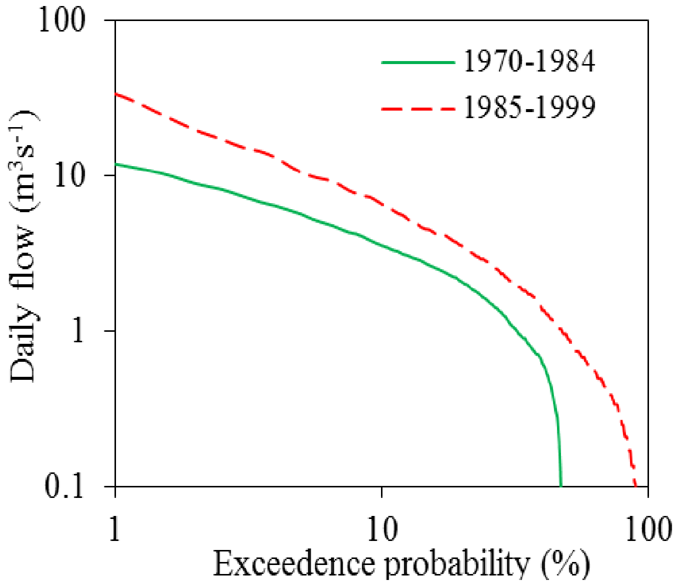

Figure 4.26: Daily flow duration curves before land use change (1970 to 1984) and after land use change (1985 to 1999) for Likangala River

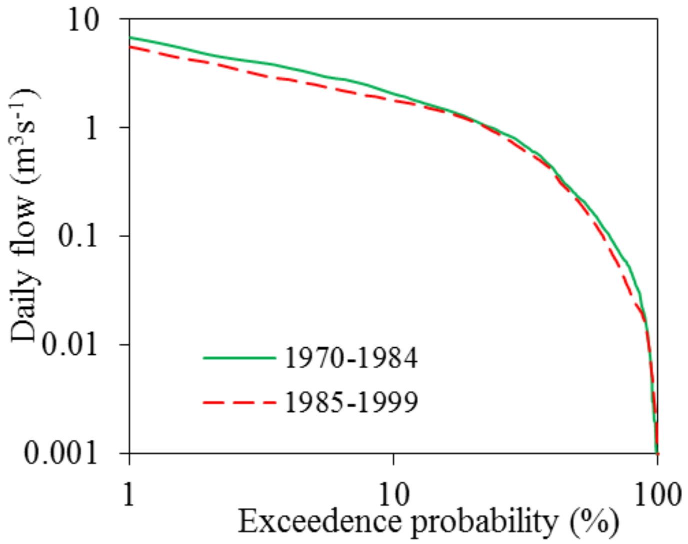

Figure 4.27: Daily flow duration curves before land use change (1970 to 1984) and after land use change (1985 to 1999) for Mulunguzi River

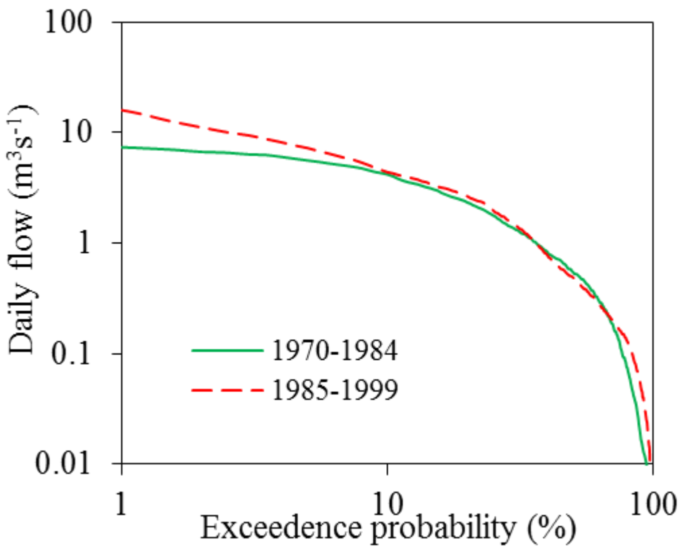

Figure 4.28: Daily flow duration curves before land use change (1970 to 1984) and after land use change (1985 to 1999) for Thondwe River

From the flow duration curves presented as log-log plots in Figures 4.25 to 4.28, it is evident that the period before land use change and after land use change exhibited different runoff characteristics. This is despite rainfall conditions for the two periods not being significantly different as shown by the daily rainfall duration curves in Figure 4.24 and from t-test results (Table 4.2). The daily FDCs showed higher flows and increased probability of occurrence in the deforested period of 1985 to 1999, particularly in the watersheds of Domasi, Likangala and Thondwe.

Considering that rainfall conditions did not significantly change between the two periods for all the four watersheds, the increased runoff characteristic could be attributed to the alteration of surface flow regimes mostly due to reduced forest vegetation and increased cultivated and bare lands in these watersheds. Cultivated crops such as maize as the case for these watersheds generally have low leaf area compared to forests or other natural vegetation and therefore less rainfall interception which often leads to more overland flow compared to forests (Costa and Foley, 1997; Zhang *et al.*, 2001; Costa *et al.*, 2003; Odongo *et al.*, 2014). The increase in runoff characteristics in the watersheds of Domasi, Likangala and Thondwe may therefore be attributed to increased overland flow from the increasing bare lands and agricultural lands.

Since maize is the predominant crop in the watersheds of Domasi, Likangala, and Thondwe, an increase in cultivated land leads to more runoff generation, especially during the first month of the rainy season when the crop is in its initial stages and the vast portion of land is exposed. For the case of Mulunguzi watershed, despite having a small size area which is expected to have significant hydrologic response to changes in land use, there was not much change in its runoff characteristic. This was particularly because its land use which was predominantly forest did not change much for the studied period. Comparing FDCs for the 1970 to 1984 and 1985 to 1999 periods, there was a small decrease in runoff tendency in the Mulunguzi watershed, which can be linked more seepage with a slight change of forest cover to grassland.

4.3 Impact of land use change on flow estimated using SWAT

4.3.1 Sensitivity analysis

Table 4.8 shows global sensitivity analysis results on the most influencing factors to flow simulation.

Table 4.8: Ranking of SWAT parameters based on sensitivity analysis

Rank	**Parameter name**	**t-stat**	***P-value***
1	ESCO	-2.8161	0.0137
2	GW_DELAY	-2.7072	0.0170
3	CN2	1.9775	0.0680
4	SOL_AWC	1.5059	0.1543
5	ALPHA_BF	1.3231	0.2070
6	CANMX	-1.0369	0.3173
7	CH_N2	-1.0295	0.3207
8	SURLAG	-0.8531	0.4080
9	EPCO	-0.6332	0.5368
10	BIOMIX	-0.5665	0.5800
11	GW_REVAP	-0.4529	0.6576
12	RCHG_DP	0.3285	0.7474
13	CH_K2	-0.2428	0.8117
14	OV_N	-0.0302	0.9763
15	SOL_BD	-0.0150	0.9883

From the results in Table 4.8, it can be seen that the five most sensitive parameters were; the soil evaporation compensation factor (ESCO), groundwater delay (GW_DELAY), SCS runoff curve number (CN2), available water content of the soil (SOL_AWC) and baseflow alpha factor (ALPHA_BF). Selection of these five parameters was based on the obtained t-stat and p-value for each parameter after the sensitivity analysis in SWAT-CUP. According to the SWAT-CUP use guide manual, the larger the absolute value of t-stat, and the smaller the *p*-value, the more sensitive the parameter (Abbaspour, 2012).

4.3.2 Calibration and validation

Table 4.9 shows the final (best) parameter values that were obtained after model calibration. The coefficient of determination (R^2) for the calibration and validation are presented in Figures 4.29 and 4.30.

Table 4.9: Final values of sensitive parameters after calibration

No	Parameter	Range	Initial value	Adjusted / last value
1	ESCO	-0.25 – 0.25	Default	+0.95
2	GW_DELAY	30 - 450	Default	+0.025
3	CN2	-0.2 – 0.2	Default	-0.02
4	SOL_AWC	0 - 1	Default	0.35
5	ALPHA_BF	0 - 1	Default	219

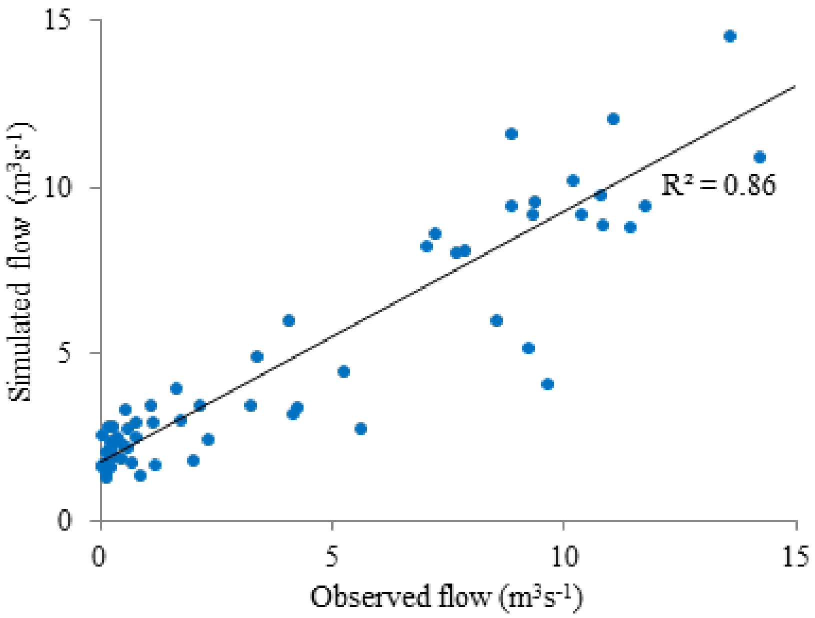

Figure 4.29: Goodness-of-fit for the calibration period of 1983 to 1987

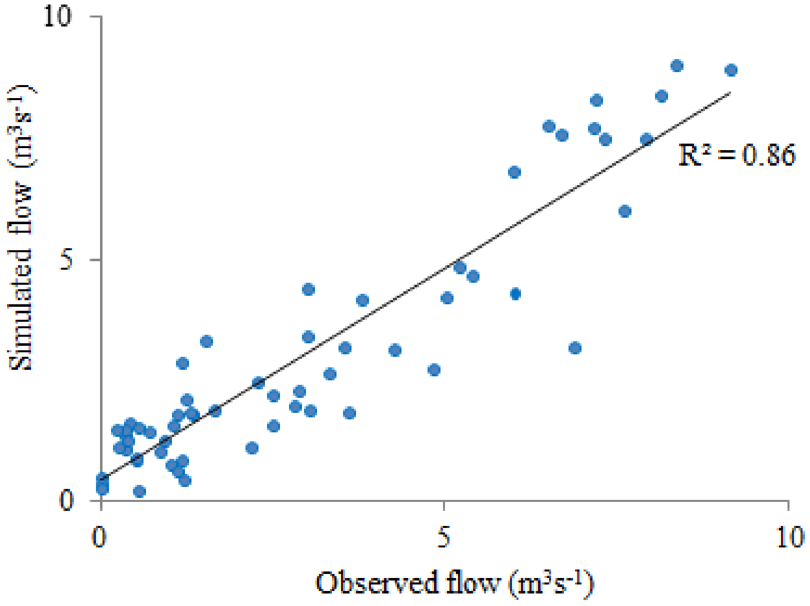

Figure 4. 30: Goodness-of-fit for the validation period of 1988 to 1992

As shown in Figures 4.29 and 4.30, the coefficient of determination (R^2) values of 0.86 and 0.86 were obtained for the calibration and validation periods respectively. These coefficients indicate that a strong relationship exists between the observed and simulated flows, both in the calibration and validation periods. A time series plot for the observed and simulated monthly streamflow for the calibrated and validated period (1983 to 1992) is presented in Figure 4.31.

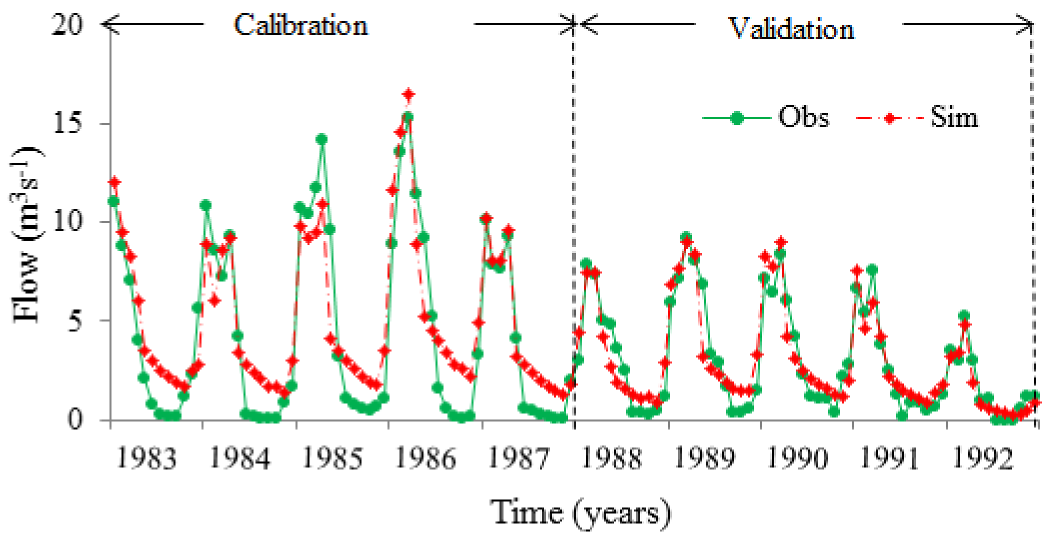

Figure 4.31: Observed and simulated monthly flow of Thondwe watershed

Table 4.10 shows the results of the model performance assessed using the Nash-Sutcliffe efficiency (NS), percent bias (PBIAS) and standard deviation ratio (RSR) for the calibration and validation.

Table 4.10: Summary statistics for the model performance indicators

Indicator	Calibration	Validation
Nash-Sutcliffe (NS)	0.83	0.81
Percent bias (PBIAS)	-13.2	-9.7
Standard deviation ratio (RSR)	0.41	0.37

From the model performance results in Table 4.10, it is evident that the model performed satisfactorily in the simulation of streamflow, both in the calibration and validation periods. According to Moriasi *et al.* (2007), a model is considered satisfactory in simulating streamflow if; NS > 0.5, PBIAS < ± 25% and RSR ≤ 0.7. In most studies however, the commonly used statistics reported for calibration and validation are the R^2 and NS (Arnold *et al.*, 2012).

4.3.3 Quantified impact of land use change and climate variability on runoff

Table 4.11 shows the simulated mean annual runoff depth (mm) under different land uses of 1973 and 1994, with other factors held constant.

Table 4.11: Simulated mean annual runoff depth for Thondwe watershed

Scenario	Land use	Climate data	Measured (mm)	Simulated (mm)	Change (mm)	Change (%)
S1	1973	1970 - 1984	410.6	461.3	-	-
S2	1994	1970 - 1984	410.6	474.8	13.5	2.9
S3	1973	1985 - 1999	355.8	399.7	-61.6	-13.3
S4	1994	1985 - 1999	355.8	405.5	-55.8	-12.1

From the results in Table 4.11, the simulated results show that a change in land use within the Thondwe watershed resulted to a subsequent increase in runoff. Compared with the simulated runoff depth under the 1973 land use (S1), the runoff depth under the 1994 land use (S2) increased by 2.9%. This increase in runoff depth may be attributed to decline in forest vegetation and grassland by about 19% and 6%, respectively; and an increase in cultivated and bare land areas by about 11% and 15%, respectively within the Thondwe watershed. This small increase in streamflow due to land use change however is generally within the bounds of uncertainty of errors associated with land use classification.

The increase in runoff despite no increase in rainfall implies reduced seepage, hence less groundwater recharge leading to declining baseflow in the long run. Findings on baseflow trends from this study for all three deforested watersheds also showed a significantly declining tendency between 1970 and 1999. Bruijnzeel (1990) observed that baseflow from deforested land may decrease if infiltration capacity is reduced, which explains the findings of this study. Other studies on the impact of changes of catchment vegetation on hydrology; such as those by Zhang *et al.* (1999), Best *et al.* (2003) and Andréassian (2004) also showed that deforestation results to an increase in mean annual discharge. These studies however were conducted on small watersheds of about $1km^2$ compared to Thondwe watershed which has a medium size of 306 km^2.

The results in Table 4.11 further show that the effect of climate variability alone (Scenario S3) reduces the mean annual runoff by 13.3% during the 1985 to 1999 period. The decrease in runoff relates to rainfall trends which tended to decrease although not significantly detected by the MK trend test at a level of significance of 0.05. Study by Siriwardena *et al.* (2006) showed that a small change in rainfall may yield a significant impact on the resulting runoff. Their study showed that while rainfall increased by 8.4% in the Comet watershed in Australia, the runoff increased by 78%. The results in Table 4.11 further show that the combined effect of land use change and climate variability was to decrease runoff by 12.1%, which is smaller than climate variability effect alone.

4.3.5 Quantified impact on soil water and evapotranspiration

Table 4.12 shows the simulated results of soil water (SW), actual evapotranspiration (ET) and potential evapotranspiration (PET) for Thondwe watershed under the four scenarios as in 4.3.4.

Table 4.12: Simulated average annual soil water and evapotranspiration for Thondwe watershed

	Land use	**Climatic data**	**Soil water**		**Evapotranspiration**		
			SW (mm)	Change (%)	ET (mm)	Change (%)	PET (mm)
S1	1973	1970 - 1984	97.7	-	368.0	-	1649.0
S2	1994	1970 - 1984	96.7	-1.0	367.7	-0.1	-
S3	1973	1985 - 1999	89.9	-8.7	355.2	-3.5	1701.5
S4	1994	1985 - 1999	89.7	-8.9	354.5	-3.7	-

As shown in Table 4.12, land use change and climate variability both decreased the soil water content in Thondwe watershed. The decrease however was more from climate variability contributing 8.7% compared to land use change contribution of 1%. The soil water decrease in turn had a similar decreasing effect on the actual evapotranspiration (ET), which is dependent on the soil moisture availability. The results also indicated enhanced potential evapotranspiration (PET) from 1649 mm to 1702 mm between the two periods analysed (Table 4.12), suggesting complimentary relationship between actual and potential evapotranspiration. Hobbins *et al.* (2004) suggested that because of the complementarity effect, higher potential evapotranspiration may only result to an increase in the actual evapotranspiration within limits of moisture availability. This may explain reasons for a decrease in the actual evapotranspiration (ET) despite increasing in the potential evapotranspiration (PET) observed in this study.

CHAPTER FIVE

CONCLUSIONS AND RECOMMENDATIONS

5.1 Conclusions

Changes in land use and climatic variations in the Lake Chilwa Basin were analysed; and their resulting impacts on streamflow were determined. From this study, it was concluded that;

1. There was an overall increase in area under agriculture from 29.2% to 41.5% between 1973 and 1994 in the Chilwa Basin. As agricultural area increased, there was a reduction of forest, bare land and wetland by 7.8%, 5.5% and 7.7%, respectively at the basin level. Grassland however increased by 7.6% over the study period. There was notable variation of Land use change in the individual watersheds. The watersheds of Domasi, Likangala and Thondwe generally experienced a significant reduction of forest vegetation and wetland areas due to increasing cultivation between 1973 and 1994. The Mulunguzi watershed however was well conserved with significant proportion of at least 96% forest area between 1973 and 1994.

2. The hydroclimatological characteristics within Lake Chilwa Basin generally changed over the study period. There was a notable delayed rainfall onset and a quick cessation observed from 1985 to 1999 compared to the 1970 to 1984 period. There was evidence of declining baseflows and increased peak flows which is synonymous with degraded watersheds that could not be explained by rainfall regime. Despite the study focus being from 1970 to 1999 due to data limitations; it was evident that there was continued degradation in the basin based on the analysis of 2013 Landsat image. Therefore, continued degradation of Lake Chilwa is likely to intensify floods and droughts during rainfall and dry seasons respectively following future projections of increased rainfall and air temperature for the region according to IPCC (2007).

3. The SWAT model performed well as shown by the NS of 0.83, PBIAS of -13.2% and RSR of 0.41. Based on the simulations, the impact of land use change in the Thondwe watershed was to increase the mean annual runoff by 3% while climate variability decreased both the mean water yield and actual evapotranspiration by 13% and 4%, respectively. Overall, climate variability influenced surface hydrology more significantly than land use change in the Thondwe watershed.

5.2 Recommendations

1. The study recommends catchment restoration in the degraded watersheds to reverse the adverse hydrological processes observed in Domasi, Likangala and Thondwe sub-watersheds and hence recover and maintain flows as is the case with Mulunguzi watershed. In addition, there should be continuous monitoring of land use change in the Lake Chilwa Basin through remote sensing techniques for better watershed management.

2. It is further recommended that the hydro-meteorological data such as streamflow and rainfall be collected at a better density network, and reliably stored in daily format. Data limitations faced in this study led to simulations being performed only for the Thondwe watershed. It is therefore recommended to extend the analysis to the other watersheds for comparison of the responses.

3. This study also recommends the use of the calibrated SWAT model to simulate scenarios that will provide knowledge of land use changes that are beneficial for improving flows in the basin. Since this study had some weather data limitations for the modelling, future studies should consider using weather data from other sources such as Climwat to model for the other watersheds.

REFERENCES

Abbaspour, K. C. (2013). SWAT-CUP 2012. *SWAT Calibration and Uncertainty Program – A User Manual*.

Abbaspour, K. C., Johnson, C. A. and Van Genuchten, M. T. (2004). Estimating uncertain flow and transport parameters using a sequential uncertainty fitting procedure. Vadose Zone Journal, 3(4): 1340-1352.

Abburu, S. and Golla, S. B. (2015). Satellite image classification methods and techniques. A review. International Journal of Computer Applications, 119(8): 129-138

Adams, H. D., Luce, C. H., Breshears, D. D., Allen, C. D., Weiler, M., Hale, V. C. and Huxman, T. E. (2012). Ecohydrological consequences of drought- and infestation-triggered tree die- off: insights and hypotheses. Ecohydrology, 5(2): 145-159.

Adnan, N. A. and Atkinson, P. M. (2010). Exploring the impact of climate and land use changes on streamflow trends in monsoon catchment. International Journal of Climatology, 31(6): 815-831.

Allan, J. D. (2004). Influence of land use and landscape setting on the ecological status of rivers. Limnetica, 23(3-4): 187-197.

Allison, E. H., Andrew, N. L. and Oliver, J. (2007). Enhancing the resilience of inland fisheries and aquaculture systems to climate change. Journal of SAT Agricultural Research, 4(1).

Andréassian, V. (2004). Water and forests: from historical controversy to scientific debate. Journal of hydrology, 291(1): 1-27.

Archer, D. (2003). Scale effects on the hydrological impact of upland afforestation and drainage using indices of flow variability: the River Irthing, England. Hydrology and Earth System Sciences Discussions, 7(3): 325-338.

Arnold, J. G., Morias, D. N., Gassman, P. W., Abbaspour, K. C., White, M. J., Srinivasan, R., Santhi, C., Harmel, R. D., van Griensven, A., van Liew, M. W., Kannan, N. and Jha, M. K. (2012). SWAT: Model use, calibration and validation. Journal of American Society of Agricultural and Biological Engineers, 55 (4): 1491-1508.

Arnold, J. G. and Fohrer, N. (2005). SWAT2000: Current capabilities and research opportunities in applied watershed modelling. Hydrological processes, 19(3): 563-572.

Arnold, J. G., Srinivasan, R., Muttiah, R. S., and Williams, J. R. (1998). Large area hydrologic modeling and assessment part I: model development. JAWRA Journal of the American Water Resources Association, 34(1): 73-89.

Bae, D. H., Jung, I. W. and Chang, H. (2008). Long- term trend of precipitation and runoff in Korean river basins. Hydrological processes, 22(14): 2644-2656.

Balascio, C. C., Palmeri, D. J. and Gao, H. (1998). Use of a genetic algorithm and multi-objective programming for calibration of a hydrologic model. Transactions of the ASAE, 41(3): 615-619.

Bárdossy, A. (2007). Calibration of hydrological model parameters for ungauged catchments. Hydrology and Earth System Sciences Discussions, 11(2): 703-710.

Bates, B. C., Kundzewicz, Z. W., Wu, and S. and Palutikof, J. P. Eds., (2008). Climate Change and Water. Technical Paper of the Intergovernmental Panel on Climate Change, IPCC Secretariat, Geneva, 210 pp.

Best, A., Zhang, L., McMahon, T., Western, A. and Vertessy R. (2003). A Critical Review of Paired Catchment Studies with Reference to the Seasonal Flows and Climate Variability. Cooperative Research Centre for Catchment Hydrology Technical Report, Monash University: Monash, Victoria.

Beven, K. and Binley, A. (1992). The future of distributed models: model calibration and uncertainty prediction. Hydrological processes, 6(3): 279-298.

Bosch, J. M. and Hewlett, J. D. (1982). A review of catchment experiments to determine the effect of vegetation changes on water yield and evapotranspiration. Journal of hydrology, 55(1-4): 3-23.

British Geological Survey. (2004). Groundwater quality: British National Environment Research Council.

Brown, A. E., Zhang, L., McMahon, T. A., Western, A. W. and Vertessy, R. A. (2005). A review of paired catchment studies for determining changes in water yield resulting from alterations in vegetation. Journal of hydrology, 310(1): 28-61.

Bruijnzeel, L. A. (1990). Hydrology of Moist Forests and the Effects of Conversion: A State of Knowledge Review, Free University, Amsterdam.

Bruijnzeel, L. A. (2004). Hydrological functions of tropical forests: not seeing the soil for the trees? Agriculture, ecosystems & environment, 104(1): 185-228.

Butt, A., Shabbir, R., Ahmad, S. and Aziz, N. (2015). Land use change mapping and analysis using Remote Sensing and GIS: A case study of Simly watershed, Islamabad, Pakistan. The Egyptian Journal of Remote Sensing and Space Science, 18(2): 251-259.

Cambien, N. (2017). Evaluation of the Soil and Water Assessment Tool (SWAT) to simulate pesticide dynamics in the Guyas River Basin (Ecuador) (Doctoral dissertation, Ghent University).

Chavula, G. (2000). The evaluation of the present and potential water resource management for the Lake Chilwa Basin. US Land Tenure Centre, University of Wisconsin. Available from: http://wisc.edu/Itc/baspusafri.html (Accessed on 21 July, 2016).

Choi, W. and Deal, B. M. (2008). Assessing hydrological impact of potential land use change through hydrological and land use change modeling for the Kishwaukee River basin (USA). Journal of Environmental Management, 88(4): 1119-1130.

Costa, M. H., Botta, A. and Cardille, J. A. (2003). Effects of large-scale changes in land cover on the discharge of the Tocantins River, Southeastern Amazonia. Journal of Hydrology, 283(1): 206-217.

Costa, M. H. and Foley, J. A. (1997). Water balance of the Amazon Basin: Dependence on vegetation cover and canopy conductance. Journal of Geophysical Research: Atmospheres, 102(D20): 23973-23989.

Décamps, H. and Naiman, R. J. (1990). The ecology and management of aquatic- terrestrial ecotones. Man and the Biosphere Series number 4.Paris: UNESCO; Carnforth, England: Parthenon.

Delgado, J. M., Apel, H., and Merz, B. (2010). Flood trends and variability in the Mekong River, Journal of Hydrological Earth Systems Science, 14: 407-418.

Durand, P., Gascuel-Odoux, C. and Cordier, M. O. (2002). Parameterisation of hydrological models: a review and lessons learned from studies of an agricultural catchment (Naizin, France). Agronomie, 22(2): 217-228.

Eckhardt, K. (2005). How to construct recursive digital filters for baseflow separation. Hydrological processes 19(2): 507-515.

Enderle, D. I. and Weih, R. C. (2005). Integrating supervised and unsupervised classification methods to develop a more accurate land cover classification. Journal of the Arkansas Academy of Science, 59: 65-73.

Falkenmark, M, and Widstrand, C. (1992). Population and Water Resources: A Delicate Balance. Population Bulletin, Population Reference Bureau.

FAO. (2015). Water scarcity; Helping to build a world without hunger. Brochure.

FAO. (2012). Gender and climate change research in agriculture and food security in rural development. Training manual.

FAO. (2007). Coping with water scarcity; Challenges of twenty-first century: World water day.

Foli, E. and Makungwa, S. (2011). Enhancing adaptation of forests and people in Africa: development of pilot cases for selected forest ecosystems in Ghana and Malawi.

Gassman, P. W., Arnold, J. J., Srinivasan, R. and Reyes, M. (2010). The worldwide use of the SWAT Model: Technological drivers, networking impacts, and simulation trends. In 21st Century Watershed Technology: Improving Water Quality and Environment Conference Proceedings, 21-24 February 2010, Universidad EARTH, Costa Rica (p. 1). American Society of Agricultural and Biological Engineers.

Government of Malawi. (2013). Water Resources: Challenges in Malawi: Malawi State of the Environment and Outlook Report (Policy Brief): Ministry of Environment and Climate Change Management.

Government of Malawi. (2008). National statistics office. Population and housing census preliminary report.

Githui, F., Gitau, W., Mutua, F. and Bauwensa, W. (2009). Climate change impact on SWAT simulated stream flow in western Kenya. International Journal of Climatology, 29: 1823-1834.

Gleick, P. (1995). Human Population and Water: To the limits in the 21st Century. Human Population and Water, Fisheries, and Coastal Areas. Washington, D.C.: American Association for the Advancement of Science Symposium.

Green, K., Kempka, D. and Lackey, L. (1994). Using remote sensing to detect and monitor land-cover and land-use change. Photogrammetric Engineering and Remote Sensing, 60(3): 331-337.

Green, W. H. and Ampt, G. A. (1911). Studies on Soil Physics. The Journal of Agricultural Science, 4(1): 1-24.

Grocic, M. and Trajkovic, S. (2013). Analysis of changes in meteorological variables using Mann Kendall and Sen’s slope estimator statistical test in Serbia. Journal of Global and Planetary Change, 100: 172-182.

Halmy, M., Gessler, P., Hicke, J. and Salem, B. (2015). Land use/land cover change detection and prediction in the north-western coastal desert of Egypt using Markov - CA. Journal of Applied Geography, 63: 101-112.

Hargreaves, G. H. and Allen, R. G. (2003). History and evaluation of Hargreaves evapotranspiration equation. Journal of Irrigation and Drainage Engineering, 129(1): 53-63.

Hirsch, R. M., Slack, J. R. and Smith, R. A. (1982). Techniques of trend analysis for monthly water quality data. Water resources research, 18(1): 107-121.

Hobbins, M. T., Ramírez, J. A. and Brown, T. C. (2004). Trends in pan evaporation and actual evapotranspiration across the conterminous US: Paradoxical or complementary? Geophysical Research Letters, 31(13).

Hollingworth, B. E. and Chiramba, T. (2005). Implementing the SADC regional strategic action plan for integrated water resources management: Lessons and best practices.

Hu, Y., Maskey, S., Uhlenbrook, S. and Zhao, H. (2011). Streamflow trends and climate linkages in the source region of the Yellow River, China. Hydrological Processes, 25:3399 - 3411.

Hurkmans, R. T. W. L., Terink, W., Uijlenhoet, R., Moors, E. J., Troch, P. A. and Verburg, P. H. (2009). Effects of land use changes on streamflow generation in the Rhine basin. Water resources research, 45(6).

Hurrell, J. and Deser, C. (2010). North Atlantic climate variability: The role of North Atlantic Oscillation. Marine Systems, 79: 231-244.

IPCC. (2001). Impacts of climate change, adaptation and vulnerability, Contribution of the working group II to the Third Assessment Report of Intergovernmental Panel on Climate Change. Cambridge University Press, Cambridge.

IPCC. (2007). Summary for Policymakers, Climate Change 2007: The Physical Science Basis. Contribution of Working Group I to the Fourth Assessment Report of the Intergovernmental Panel. Cambridge University Press, Cambridge.

IPCC. (2013). Climate change 2013: the physical science basis: Working Group I contribution to the Fifth assessment report of the Intergovernmental Panel on Climate Change. Cambridge University Press, Cambridge

Janssen, L. and Gorte, B. (2004). Principles of remote sensing. Enschede, Netherlands: The International Institute for Geo-Information Science and Earth Observation (ICT).

Jensen, J. and Toll, D. (1982). Detecting residential land use development at the urban fringe. Photogrammetry Engineering and Remote Sensing, 48: 629 - 643.

Jipp, P. H., Nepstad, D. C., Cassel, D. K. and De Carvalho, C. R. (1998). Deep soil moisture storage and transpiration in forests and pastures of seasonally-dry Amazonia. In Potential Impacts of Climate Change on Tropical Forest Ecosystems. Springer, Netherlands.

Jovanovic, N. and Israel, S. (2012). Critical review of methods for the estimation of actual evapotranspiration in hydrological models. In *Evapotranspiration-Remote Sensing and Modeling*. InTech. Stellenbosch, South Africa.

Kafumbata, D., Jamu, D. and Chiotha, S. (2014). Riparian ecosystem resilience and livelihood strategies under test: lessons from Lake Chilwa in Malawi and other lakes in Africa. *Philosophical Transactions of Royal Society B,* 369.

Kahya, E. and Kalayci, S. (2004). Trend analysis of streamflow in Turkey. *Journal of Hydrology,* 289: 128 - 144.

Kiersch, B. (2000). Land use impacts on water resources: a literature review. Land and Water Development Division, FAO, Rome.

King, J. and Brown, C. (2006). Environmental flows: Striking the balance between development and resource protection. *Journal of Ecology and Society,* 11(2): 26-35.

Koch, M. and Cherie, N. (2013). SWAT- Modelling of the impact of future climate change on the hydrology and water resources in the Upper Blue Nile River Basin, Ethiopia. DOI: 10.5675/ICWRER.

Krause, P., Boyle, D. P. and Bäse, F. (2005). Comparison of different efficiency criteria for hydrological model assessment. *Advances in geosciences,* 5: 89-97.

Kuczera, G. and Parent, E. (1998). Monte Carlo assessment of parameter uncertainty in conceptual catchment models: the Metropolis algorithm. *Journal of Hydrology,* 211(1): 69-85.

Kumambala, P. (2010). *Sustainability of water resources development for Malawi with particular emphasis on North and Central Malawi* (Doctoral thesis, University of Glasgow, United Kingdom). Thesis retrieved from http://thesis.gla.ac.uk/1801/.

Lahmer, W., Pfützner, B. and Becker, A. (2001). Assessment of land use and climate change impacts on the mesoscale. *Physics and Chemistry of the Earth, Part B: Hydrology, Oceans and Atmosphere*, 26(7-8): 565-575.

Lal, R. (1987). *Tropical ecology and physical edaphology* (No. 574.52623 L193t). Wiley, London, GB.

Li, Z., Liu, W. Z., Zhang, X. C. and Zheng, F. L. (2009). Impacts of land use change and climate variability on hydrology in an agricultural catchment on the Loess Plateau of China. *Journal of hydrology*, 377(1): 35-42.

Ma, C., Sun, L., Liu, S., Shao, M. A. and Luo, Y. (2015). Impact of climate change on the streamflow in the glacierized Chu River basin, Central Asia. *Journal of Arid Land*, 7(4): 501-513.

Ma, L., Ahuja, L. R., Nolan, B. T., Malone, R. W., Trout, T. J. and Qi, Z. (2012). Root zone water quality model (RZWQM2): model use, calibration, and validation. *Transactions of the ASABE*, 55(4): 1425-1446.

Magoma, D. M. (2009). Hydrological modeling using SWAT in wetland catchments: Case study of Rugezi Watershed in Rwanda, First annual Nile Basin research conference, Dar es Salaam, Tanzania.

Martin, L. (1986). Change detection in the urban fringe employing Landsat satellite imagery. *Plan Canada,* 26 (7): 182 - 190.

Miller, S., Kepper, W., Mehaffey, M., Hemandez, M., Miller, R., Goodrich, D., Dovonald, K., Heggem, D. and Miller, W. (2002). Integrating landscape assessment and hydrological modelling for land cover change analysis. *Journal of American Water Resources Association,* 38(4):915-929.

Mindle, I., Kowero, G., Ngugi, D. and Luhanga, J. (2001). Agricultural land expansion and deforestation in Malawi. *Forests Trees and Livelihoods,* 11 (2): 167-182.

Montanari, L., Sivapalan, M. and Montanari, A. (2006). Investigation of dominant hydrological process in a tropical catchment in monsoonal climate via the download approach. *Journal of Hydrology and Earth System Sciences,* 10: 769 - 782.

Moriasi, D. N., Arnold, J. G., Van Liew, M. W., Bingner, R. L., Harmel, R. D. and Veith, T. L. (2007). Model evaluation guidelines for systematic quantification of accuracy in watershed simulations. *ASABE* 50 (3), 885-900.

Mumeka, A. (1986). Effect of deforestation and subsistence agriculture on runoff of the Kafue River headwaters, Zambia. *Hydrological sciences journal*, 31(4): 543-554.

Munyaneza, O. (2014). *Space - time variation of hydrological processes in Rwanda. Focus on Magina Catchment* (Doctoral Thesis, UNESCO – IHE of water education).

Mvula, P. Kalindekafe, M., Kishindo, P., Berge, E. and Njaya, F. (2014). Towards defragmenting the management system of Lake Chilwa Basin, Malawi. Peter Lang Ltd, Switzerland.

Nash, J. E. and Sutcliffe, J. V. (1970). River flow forecasting through conceptual models part I- A discussion of principles. *Journal of hydrology*, 10(3): 282-290.

Neitsch, S. L., Arnold, J. G., Kiniry, J. R., Williams, J. R. and King, K. W. (2005). Soil and water assessment tool theoretical documentation. Grassland. Soil and Water Research Laboratory, Temple, TX.

Ngongondo, C., Xu, C., Tallaksen, L., Alemaw, B. and Chirwa, T. (2011). Regional frequency analysis of rainfall extremes in the Southern Malawi using the L-moments approaches. *Stochastic Environmental Research and Risk Assessment.* DOI 10.1007/s00477-011-0480-x.

Njaya, F., Snyder, K. A., Jamu, D., Wilson, J., Howard-Williams, C., Allison, E. H. and Andrew, N. L. (2011). The natural history and fisheries ecology of Lake Chilwa, southern Malawi. *Journal of Great Lakes Research*, 37: 15-25.

Odongo, V. O., Mulatu, D. W., Muthoni, F. K., Van Oel, P. R., Meins, F. M., Van der Tol, C., Skidmore, A. K., Groen, T. A., Becht, R., Onyando, J. O. and van der Veen, A. (2014). Coupling socio-economic factors and eco-hydrological processes using a cascade-modeling approach. Journal of hydrology, 518: 49-59.

Odongo, V. O., Tol, C., Oel, P. R., Meins, F. M., Becht, R., Onyando, J. and Su, Z. (2015). Characterisation of hydroclimatological trends and variability in the Lake Naivasha basin, Kenya. *Hydrological Processes*, 29(15): 3276-3293.

Ozesmi, S. and Bauer, M. (2002). Satellite remote sensing of wetlands. *Wetlands Ecology and Management*, 10(5): 381 - 402.

Palamuleni, L. G., Ndomba, P. M. and Annegarn, H. J. (2011). Evaluating land cover change and its impact on hydrological regime in Upper Shire river catchment, Malawi. *Regional Environmental Change*, 11(4): 845-855.

Phalombe District Commissioner, (2014). District state of the environment and outlook report.

Principe, J. and Blanco, A. (2013). SWAT Model for assessment of climate change and land use or land cover change impacts on Philippine soil loss and exploration of land cover-based mitigation measures: Case of Cagayan River Basin.

Rayne, S. and Forest, K. (2013). The decline of global per capita renewable internal freshwater resources. *Sask: Saskatchewan Institute of Applied Sciences*.

Refsgaard, J. C. (1997). Parameterisation, calibration and validation of distributed hydrological models. *Journal of hydrology*, 198(1): 69-97.

Refsgaard, J. C., Storm, B. and Clausen, T. (2010). Système Hydrologique Europeén (SHE): review and perspectives after 30 years development in distributed physically-based hydrological modelling. *Hydrology Research*, 41(5): 355-377.

Rouholahnejad, E., Abbaspour, K. C., Vejdani, M., Srinivasan, R., Schulin, R. and Lehmann, A. (2012). A parallelization framework for calibration of hydrological models. *Environmental Modelling & Software*, 31: 28-36.

Sang, J. K. (2005). Modelling the impact of changes in land use, climate and reservoir storage on flooding in the Nyando basin (Doctoral dissertation, Masters thesis submitted to Biomechanical and Environmental Engineering Department, Jomo Kenyatta University of Agriculture and Technology, Kenya).

Sharif, M. and Burn, D. (2009). Detection of linkages between extreme flow measures and climate indices. *World academy of science, engineering and technology*, 60: 871-876.

Short, N. M. (2005). Image processing and interpretation [online]. http://www.fas.org/irp/imint/docs/rst/Sect1/Sect1_16.html (Accessed 6 September 2016).

Siriwardena, L., Finlayson, B. L. and McMahon, T. A. (2006). The impact of land use change on catchment hydrology in large catchments: The Comet River, Central Queensland, Australia. *Journal of Hydrology,* 326 (2006): 199 - 214.

Sophocleous, M. (2002). Interactions between groundwater and surface water: the state of the science. *Hydrogeology journal*, 10(1): 52-67.

Svennson, C., Hannaford, J., Kundzewicz, Z. and Marsh, T. (2006). Trends in river floods: why is there no clear signal in observations? *Research Centre of Agricultural and Forest Environment, Polish Academy of Sciences, Bukowska,* 19: 60-809.

Tian, P., Zhao, G., Li, J. and Tian, K. (2011). Extreme value analysis of streamflow time series in Poyang Lake Basin, China. *Water Science and Engineering*, 4(2): 121-132.

Trucano, T. G., Swiler, L. P., Igusa, T., Oberkampf, W. L. and Pilch, M. (2006). Calibration, validation, and sensitivity analysis: What's what. *Reliability Engineering & System Safety*, 91(10): 1331-1357.

USACE. (2009). Hydrologic modeling system HEC-HMS user's manual. (http://www.hec.usace.army.mil/software/hec-hms/) (Accessed February 17, 2018).

USACE. (2000). HEC-HMS hydrologic modeling system user's manual. Hydrologic Engineering Center, Davis, California.

USDA, Soil Conservation Service. (1972). National Engineering Handbook, Section 4: Hydrology. Washington, DC.

Van Griensven, A. and Bauwens, W. (2003). Multiobjective autocalibration for semi-distributed water quality models. *Water Resources Research*, 39(12): 1348-1356.

Van Griensven, A. and Meixner, T. (2006). Methods to quantify and identify the sources of uncertainty for river basin water quality models. *Water Science and Technology*, 53(1): 51-59.

Van Liew, M. W., Arnold, J. G., and Bosch, D. D. (2005). Problems and potential of auto calibrating a hydrologic model. *Trans. ASAE*, 48(3): 1025-1040.

Varga, M., Balogh, S. and Csukas, B. (2016). GIS based generation of dynamic hydrological and land patch simulation models for rural watershed areas. *Information Processing in Agriculture*, *3*(1): 1-16.

Veith, T. L. and Ghebremichael, L.T. (2009). How to applying and interpreting the SWAT Auto calibration tools. In: Proceedings of the 5th International SWAT Conference, August 5-7, 2009, Boulder, CO.

Wang, G. X., Zhang, Y., Liu, G. and Chen, L. (2006). Impact of land-use change on hydrological processes in the Maying River basin, China. Science in China Series D: *Earth Sciences,* 49 (10): 1098-1110.

Xia, J., Wang, Z., Wang, G. and Tan, G. (2004). The renewability of water resources and its quantification in the Yellow River Basin, China. *Hydrological Processes*, 18(12): 2327-2336.

Yilmaz, A. G., Imteaz, M. A. and Ogwuda, O. (2011). Accuracy of HEC-HMS and LBRM models in simulating snow runoffs in Upper Euphrates Basin. *Journal of Hydrologic Engineering*, 17(2): 342-347.

Zhang, A., Zhang, C., Fu, G., Wang, B., Bao, Z. and Zheng, H. (2012). Assessments of impacts of climate change and human activities on runoff with SWAT for the Huifa River Basin, Northeast China. *Water resources management*, 26(8): 2199-2217.

Zhang, L., Dawes, W. R. and Walker, G. R. (2001). Response of mean annual evapotranspiration to vegetation changes at catchment scale. *Water resources research*, *37*(3), 701-708.

Zhang, L., Walker, G. R., and Dawes, W. (1999). Predicting the effect of vegetation changes on catchment average water balance. Technical report 99/12, 35pp.

Zhang, X., Zhang, L., Zhao, J., Rustomji, P. and Hairsine, P. (2008). Responses of streamflow to changes in climate and land use/cover in the Loess Plateau, China. *Water Resources Research*, 44(7): 1-12.

APPENDICES

APPENDIX A

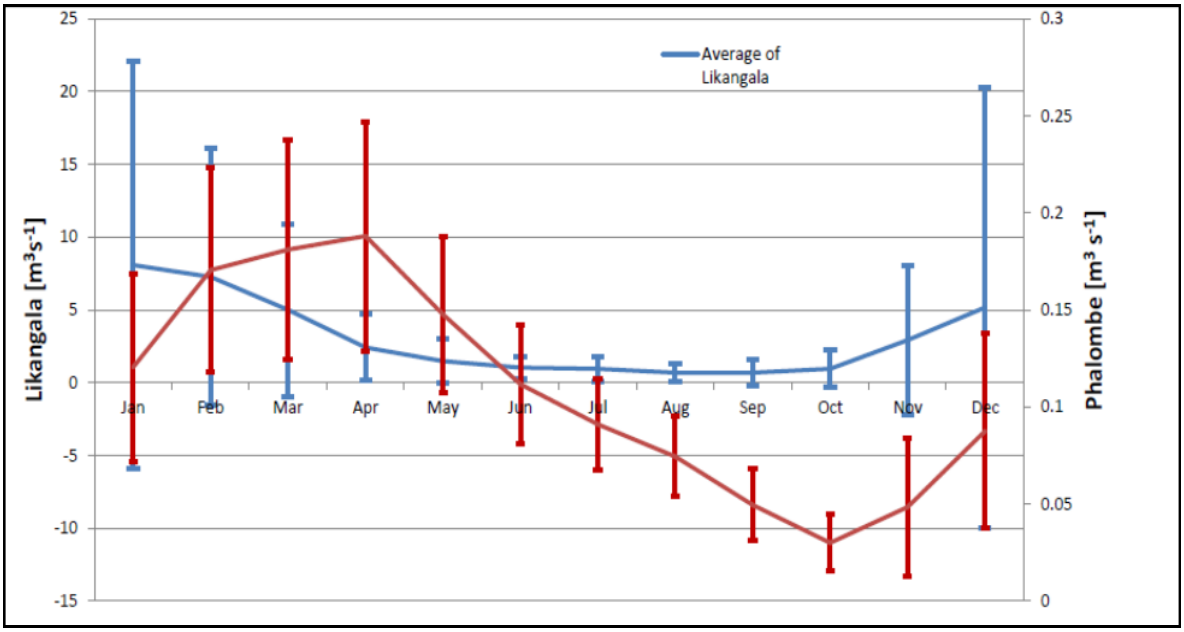

A1: Streamflow seasonality pattern

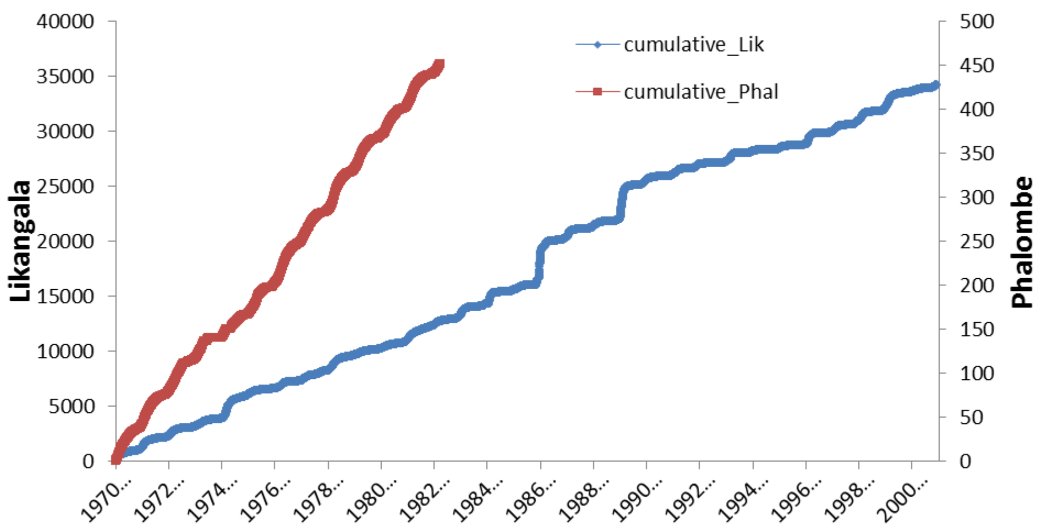

A4: Single curve analysis for Likangala and Phalombe Rivers

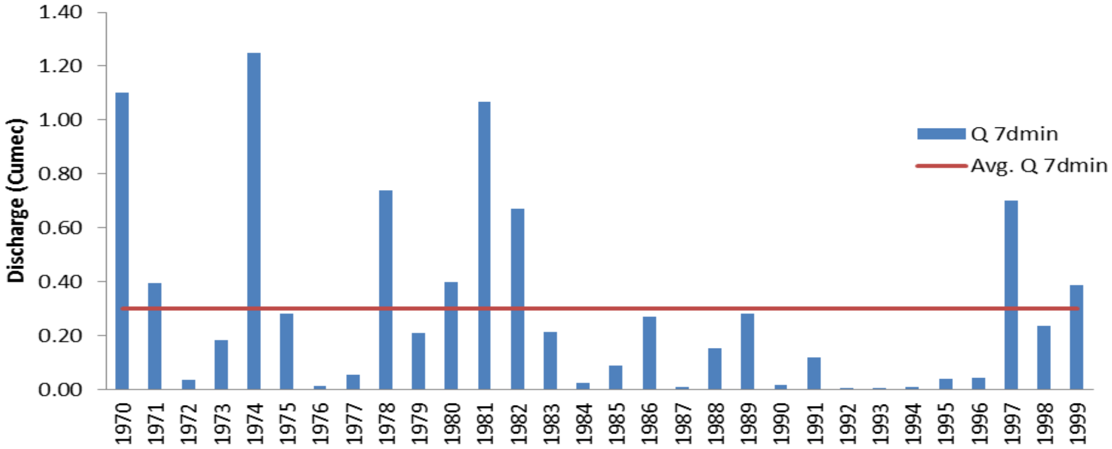

A7: Minimum flows (Q 7_{dmin}) - Likangala River

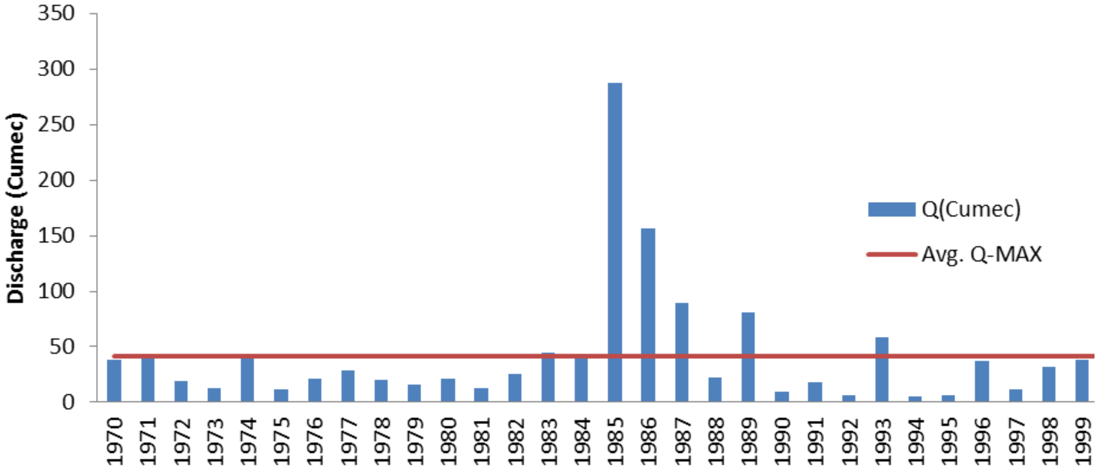

A8: Maximum flows (*AMS - 5*) - Likangala River

APPENDIX B

B1: Streamflow gauging point-coordinates, data gaps and watershed area

Station ID	Station name	Station coordinates		Period	Watershed area (km^2)
H1	Domasi TTC	758246	8309299	1970-99	75
H3	Nkokanguwo	747509	8295480	1970-99	144
H2	Zomba Plateau	747537	8300863	1970-99	18
H4	Jali	748156	8295355	1970-99	306

B2: Rainfall gauging point ID codes and coordinates

Station ID	Station name	Station coordinates		Data period	Watershed
P1	Domasi College	758246	8309299	1970-99	Domasi
P3	Chancellor College	747509	8295480	1970-99	Likangala
P2	Zomba Plateau	747537	8300863	1970-99	Mulunguzi
P5	Makoka	748156	8295355	1970-99	Thondwe

APPENDIX C

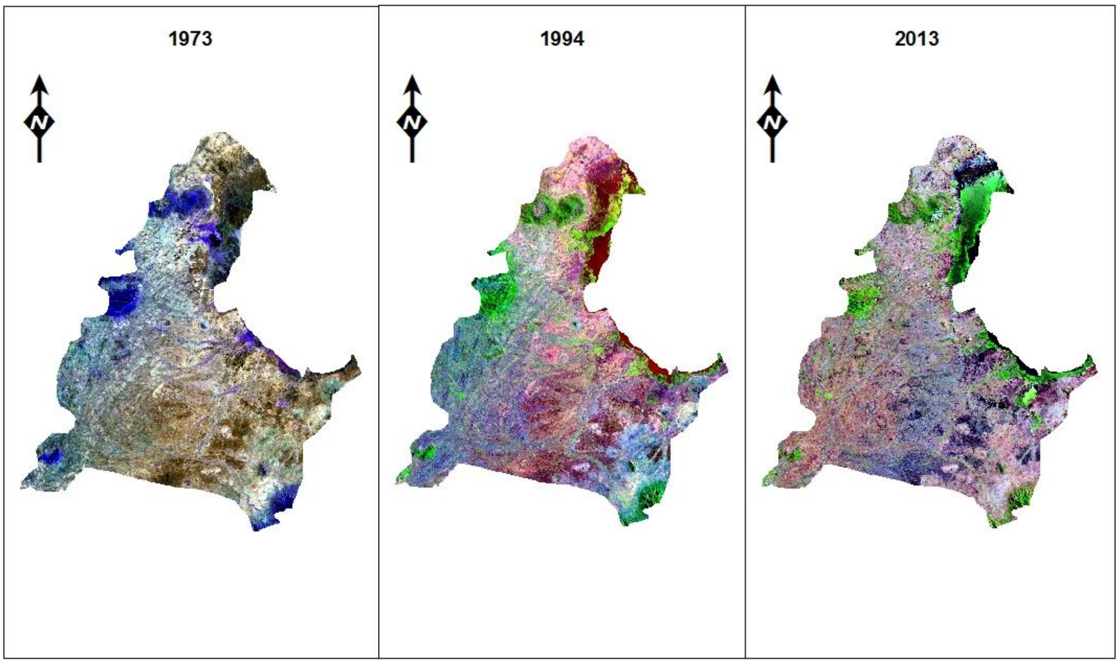

C1: Lake Chilwa Basin colour composites: 1973, 1994 and 2013

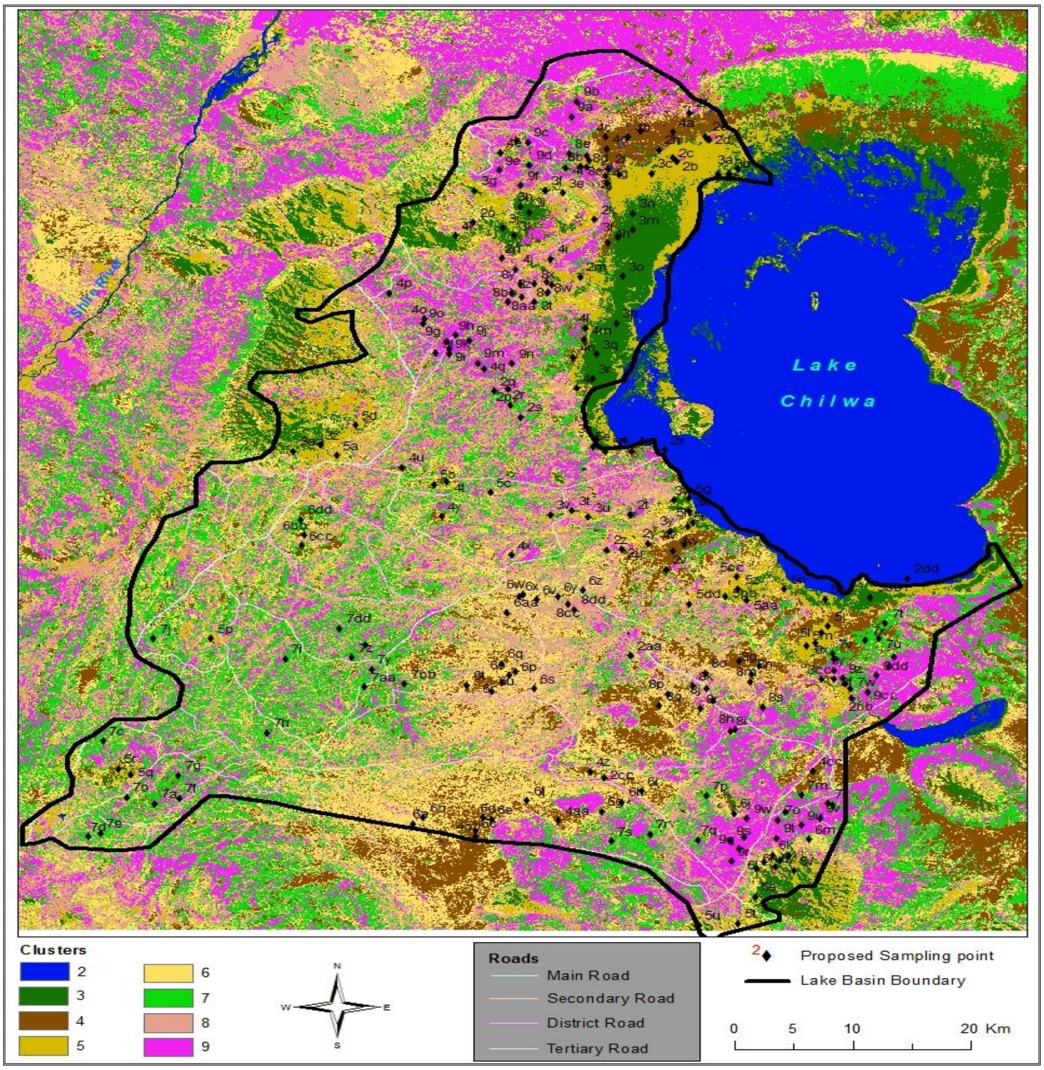

C2: Map of Lake Chilwa used for groundtruthing

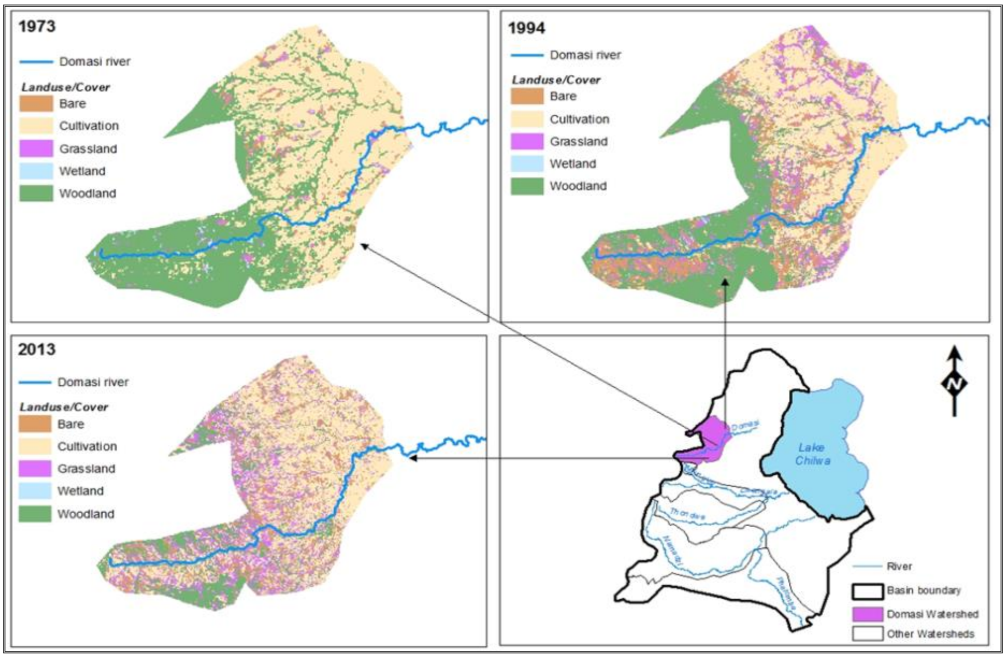

C3: Land use change map for Domasi Watershed (1973, 1994 and 2013)

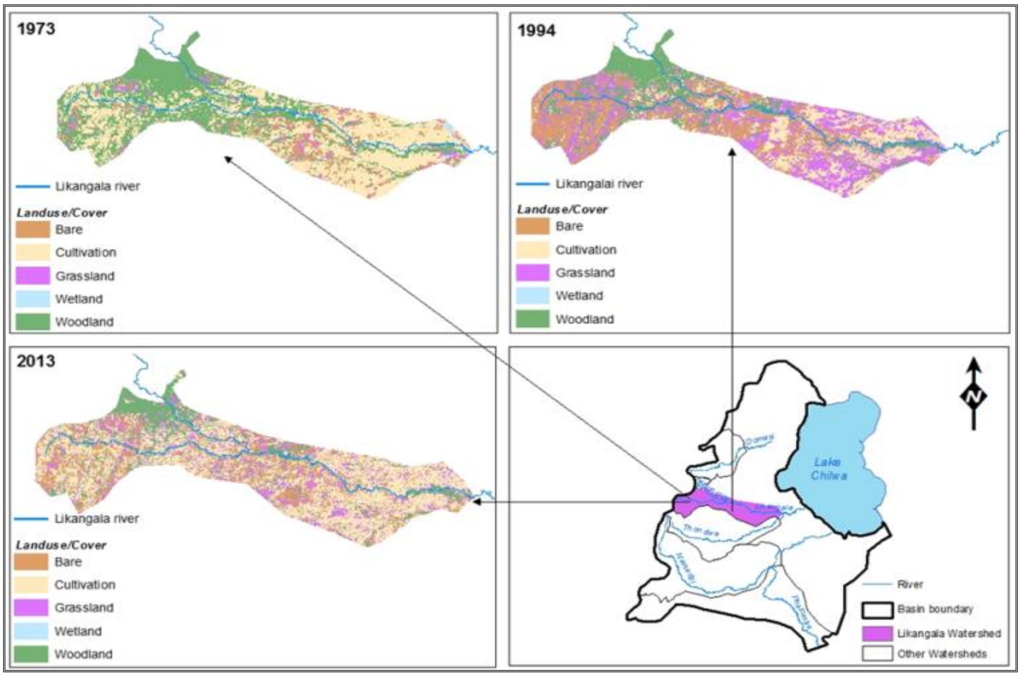

C4: Land use change map for Likangala Watershed (1973, 1994 and 2013)

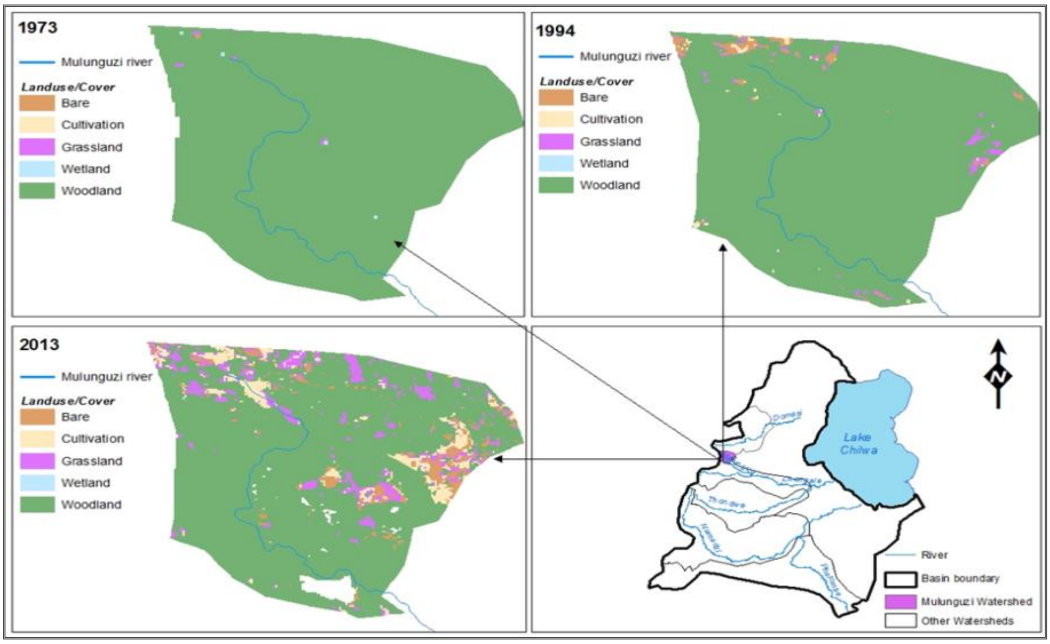

C5: Land use change map for Mulunguzi Watershed (1973, 1994 and 2013)

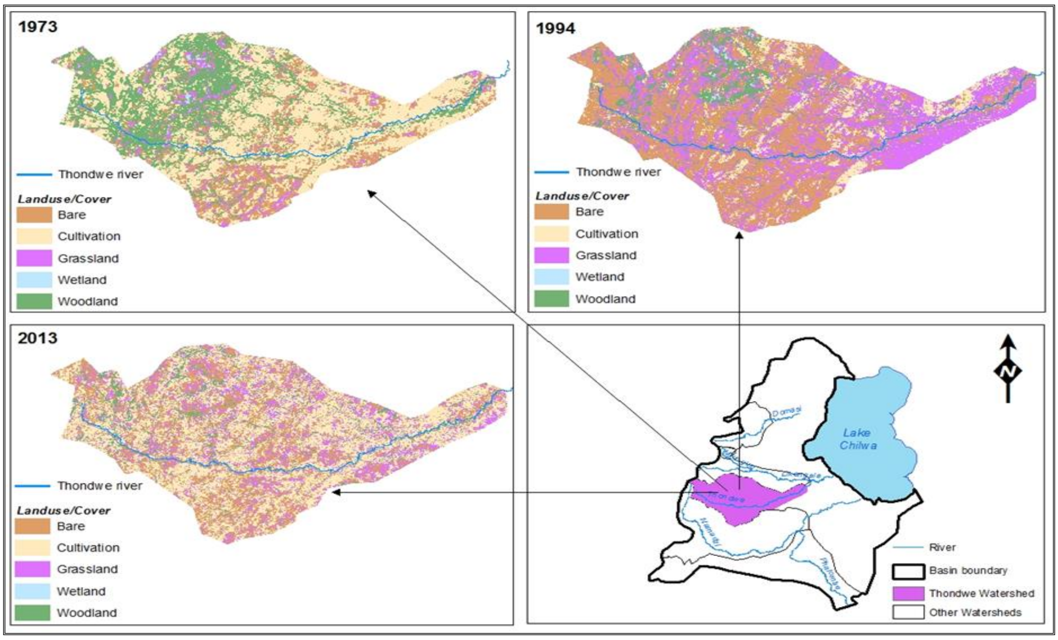

C6: Land use change map for Thondwe River Watershed (1973, 1994 and 2013)

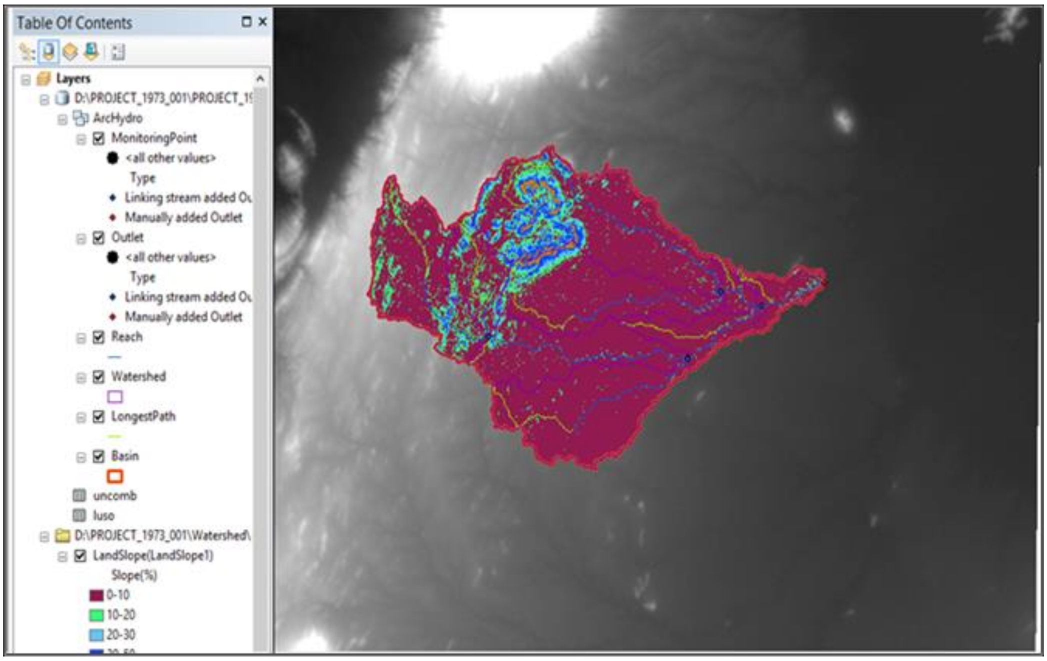

C7: Land use, soil and slope overlay

APPENDIX D

D1: Land use change in the watersheds of Domasi, Likangala, Mulunguzi and Thondwe

Watershed	Year	Area	Bare land	Cultivation	Grassland	Wetland	Forest
Domasi	1973	km^2	7.8	57.4	23.1	1.3	70.8
		Percent	4.8	35.8	14.4	0.8	44.1
	1994	km^2	25.2	60.3	19.1	0.7	55.1
		Percent	15.7	37.6	11.9	0.5	34.4
	2013	km^2	23.6	78.5	30.2	0.1	28.0
		Percent	14.7	48.9	18.8	0.08	17.4
Likangala	1973	km^2	32.1	84.2	7.5	2.0	78.4
		Percent	15.8	41.3	3.7	1.0	38.4
	1994	km^2	56.1	94.0	8.9	0.6	44.6
		Percent	27.5	46.1	4.3	0.3	21.8
	2013	km^2	41.7	126.7	1.0	0.1	34.6
		Percent	20.4	62.1	0.5	0.1	17.0
Mulunguzi	1973	km^2	0.0	0.0	0.02	0.01	16.7
		Percent	0.0	0.0	0.2	0.1	99.7
	1994	km^2	0.03	0.02	0.5	0.06	16.3
		Percent	0.2	0.1	2.8	0.0	96.9
	2013	km^2	0.7	1.1	1.1	0.0	13.9
		Percent	4.0	6.7	6.7	0.0	82.6
Thondwe	1973	km^2	55.9	132.6	19.4	2.5	97.9
		Percent	18.1	43.0	6.3	0.8	31.8
	1994	km^2	101.9	164.1	0.0	3.6	38.6
		Percent	33.0	53.6	0.0	0.5	12.5
	2013	km^2	67.7	185.5	25.2	0.1	29.7
		Percent	22.0	60.2	8.2	0.1	9.6

D2: Chancellor College annual precipitation t-test results, α = 0.05

	1970-84	**1985-99**
Mean	1384.4	1384.6
Variance	62187.1	208292.6
Observations	15.0	15.0
Pooled Variance	135239.8	
Hypothesized Mean Difference	0.0	
df	28.0	
t Stat	0.0016	
t Critical two-tail	2.0484	

D3: Domasi College annual precipitation t-test results, α = 0.05

	1970-84	**1985-99**
Mean	1315.1	1184.7
Variance	143833.5	176014.2
Observations	15.0	15.0
Pooled Variance	159923.9	
Hypothesized Mean Difference	0.0	
df	28.0	
t Stat	0.8924	
t Critical two-tail	2.0484	

D4: Makoka Research annual precipitation t-test results, α = 0.05

	1970-84	**1985-99**
Mean	866.2	992.9
Variance	91417.1	88357.1
Observations	15.0	15.0
Pooled Variance	89887.1	
Hypothesized Mean Difference	0.0	
df	28.0	
t Stat	1.1575	
t Critical two-tail	2.0484	

D5: Zomba Plateau annual precipitation t-test results, α = 0.05

	1970-84	**1985-99**
Mean	2066.2	1802.3
Variance	380840.4	184296.5
Observations	15.0	15.0
Pooled Variance	282568.5	
Hypothesized Mean Difference	0.0	
t Stat	1.3593	
t Critical two-tail	2.0484	

D6: t-test results of average river discharge for Domasi River, α = 0.05

	1970-84	**1985-99**
Mean	2.6	2.2
Variance	2.5	3.4
Observations	15.0	15.0
Pooled Variance	3.0	
Hypothesized Mean Difference	0.0	
df	28.0	
t Stat	0.5193	
t Critical two-tail	2.0484	

D7: t-test results of average river discharge for Likangala River, α = 0.05

	1970-84	**1985-99**
Mean	2.8	3.2
Variance	1.3	5.2
Observations	15.0	15.0
Pooled Variance	3.3	
Hypothesized Mean Difference	0.0	
df	28.0	
t Stat	0.5298	
t Critical two-tail	2.0484	

D8: t-test results of average river discharge for Mulunguzi River, α = 0.05

	1970-84	**1985-99**
Mean	0.9	0.8
Variance	0.3	0.3
Observations	15.0	15.0
Pooled Variance	0.3	
Hypothesized Mean Difference	0.0	
df	28.0	
t Stat	0.6651	
t Critical two-tail	2.0484	

D9: t-test results of average river discharge for Thondwe River, α = 0.05

	1970-84	**1985-99**
Mean	2.0	1.4
Variance	1.2	1.1
Observations	15	15.0
Pooled Variance	1.1	
Hypothesized Mean Difference	0.0	
df	28.0	
t Stat	1.4656	
t Critical two-tail	2.0484	

D10: Land use look-up table for 1973 map

Value,"Landuse"
196,SWRN
460,WETN
285,RNGE
1,AGRC
671,FRSD

D11: Land use look-up table for 1994 map

Value,"Landuse"
763,AGRC
1023,SWRN
836,WATR
453,WETN
881,SWRN
1128,AGRC
1098,FRSD
946,AGRC
1,AGRC
219,AGRC
630,FRSD
532,AGRC

D12: Soils look-up table

Value,"Name"
1,Je51-2/3a
4,I-Bc-c
7,Ne54-2/3b